MARMARA UNIVERSITY
FACULTY OF ENGINEERING

HIGH FIDELITY COMPUTATION OF AIR-INTAKE RELATED DRAG FORCES

REGAİB FURKAN KILIÇ

GRADUATION PROJECT REPORT
Department of Mechanical Engineering

Supervisor
Prof. Dr. Emre ALPMAN

ISTANBUL,

2021

MARMARA UNIVERSITY
FACULTY OF ENGINEERING

HIGH FIDELITY COMPUTATION OF AIR-INTAKE RELATED DRAG FORCES

by

Regaib Furkan KILIÇ

June 30,2021.

Istanbul

SUBMITTED TO THE DEPARTMENT OF MECHANICAL ENGINEERING IN PARTIAL FULFILLMENT OF THE REQUIREMENTS FOR THE DEGREE

OF

BACHELOR OF SCIENCE

AT

MARMARA UNIVERSITY

Signature of Author(s) .....Regaib Furkan KILIÇ.....

Department of Mechanical Engineering

Certified By .....

Project Supervisor, Department of Mechanical Engineering

Accepted By .....

Head of the Department of Mechanical Engineering

Acknowledgement

First of all, I would like to thank Prof. Dr. Emre ALPMAN for being my advisor on this graduation project. The time and resources provided to me by him was invaluable and much appreciated. I have truly learned a lot through this research which was only possible due to the effort put in by my advisor.

June 2021 Regaib Furkan KILIÇ

Aileme ve bütün sevdiklerime,

Contents

Symbols

C_D **:** Coefficient of Drag

C_L **:** Coefficient of Lift

μ **:** Kinematic Viscosity

ρ **:** Air Density

P_0, P_0 **:** Stagnation (Total) Pressure

P_s, P_s **:** Static Pressure

T_0, T_0 **:** Stagnation (Total) Temperature

T_s, T_s **:** Static Temperature

K **:** Kelvin

Pa **:** Pascal

N **:** Newton

m **:** Meter

ε **:** Epsilon

s **:** Second

Abbreviations

CFD: Computational Fluid Dynamics

D: Drag Force

SST: The shear stress transfer (SST)

AGARD: The Advisory Group for Aerospace Research and Development

CAD: Computer Aided Design

FVM: Finite volume method

NACA: National Advisory Committee for Aeronautics

RAE: Royal aircraft establishment

AoA: Angle of Attack

CV: Control volume

FEM: Finite element method

L: Lift Force

List of Figures

PAGE

List of Tables

PAGE

Abstract

High Fidelity Computation of Air-Intake Related Drag Forces

In this report includes three different flight conditions and their different mass flow rates of air according to drag force analysis. The drag forces due to the air intake vary considerably depending on both the flight conditions and the amount of air drawn by the engine. Accurate calculation of these forces with CFD method both affects the design process of the air intake, and it has an important share on the overall performance of the aircraft.

1. Introduction

In aviation, four different methods are used when making aerodynamic design of a product. These are analytical calculations, finite volume method (FVM) calculations, wind tunnel tests and flight tests. Analytical calculations generally consist of theoretical and empirical methods made up of designs made throughout history. Although this method's cost is very low, its uncertainty is high. For this reason, analytical calculations generally constitute the first stage of the design and are used in the calculation of the first dimensioning. Finite volume method calculations are used to model flight and wind tunnel conditions. FVM is much lower in cost than wind tunnel and flight tests, but it has a high accuracy. Wind tunnel and flight tests of the design made with FVM are performed. Then, by improving the wind tunnel and flight test results and FVM analysis, this cycle process continues until the desired performances from the design are achieved and the design reaches its final state [1].

In this graduate report, the drag forces of the pitot air intake used in military jet trainers for different flight conditions were investigated by computational fluid dynamics modeling with the finite element method. The initial dimensions of the design were determined by literature research and the pitot type air intake of the T45-Goshawk aircraft was selected. The key part of the project is when making analysis, controlling the amount of air drawn by the engine.

The drag forces due to the air inlet vary significantly depending on the flight conditions and the amount of air drawn by the engine. The proper and high-fidelity calculation of these forces using the CFD approach has a substantial impact on the air intake design process as well as the aircraft's overall performance. For this reason, entry design is remarkable in the design phase of a plane.

1.1 Purpose of the Thesis

The aim of this thesis is to make comparisons based on the amount of air drawn by the engine on the subsonic pitot type air intake using computational fluid dynamics (CFD) and examine its effects on performance. Within the scope of this project study, it is aimed to have knowledge and experience about the aerodynamic design processes of a geometry. At the same time performing experimental work with CAD and CFD systems aimed to provide work for the general performance of the aircraft.

1.2 Literature review

There are different terms used in aviation. Inside the project's parameters, literature research was conducted on high fidelity computation, air-intake, drag forces and selection of air intake and aircraft.

1.2.1 High fidelity computation

High fidelity computation is key portion of this report. There are three basic approaches to calculate the turbulent flow which are Direct numerical solution (DNS), Large Eddy Simulation (LES), lastly Reynold's Average Navier's Stoke Simulation (RANS) and their various turbulence models. One equation model Spalart – Allmaras. Two equation models k–ε family (Standard, RNG, Realizable*) k–ω family (Standard, BSL, SST*) and Reynolds Stress Models (RSM). Each model has its own advantages and cannot make every analysis. Therefore, determining the model is extremely important to make a healthy analysis.

1.2.2 What is air-intake?

Air inlet is a vital component for all turbine engines. Air inlet is an aircraft engine element used by the air taken from the atmosphere and transfers it to the compressor to reach the engine. The airflow is taken to the engine from the freestream and provides adequate ratio of pressure recovery and air deceleration. Normally, the air-inlet duct is considered an airframe part and not a part of the engine. However, the duct is very important to the engine's overall performance these features are vital to the performance and stability of the engine's operation and the engine's ability to produce an optimum amount of thrust. The air flow is taken from the inlet to the engine and ensures total pressure conservation and slowing of the flow at an appropriate rate to the compressor to reach the engine face. These properties are vital to the engine's operating performance and stability. Depending on the air intake design and the type of installation, this air flow may pass over the fuselage before properly entering the entrance. Correct type of intake and associated input geometry have important consequences in any aircraft design. Therefore, air intake design is one of the most important factors considered in the design phase of an airplane.

1.2.3 Drag Forces

Drag is an unavoidable consequence of an object moving through a fluid. Drag is the force generated parallel and in opposition to the direction of travel for an object moving through a fluid. Drag force is the resistance force caused by the motion of a body through a fluid. A drag force acts opposite to the direction of the oncoming flow velocity. This is the relative velocity between the body and the fluid.

In this report drag force was used as a performance parameter. The lower the drag force (D), the higher the thrust force of the engine, so the decrease in the drag force will increase the performance of the engine. D is calculated by the downstream component of the pressure and viscous forces on the lip and diffuser walls.

1.2.4 Air intake selection

The main purpose of an Air Intake is to slow the airflow from supersonic flight speed to subsonic speed before it enters the engine. The air intake is that part of an aircraft structure by means of which the aircraft engine is supplied with air taken from the outside atmosphere. The pitot entrance is simply a forward-facing hole. It works very well at subsonic speeds and very high at low supersonic speeds. Also called "normal shock absorption" when used for supersonic flight. Pitot air intake consists of lip and diffuser parts.

The purpose of the Pitot Type air intake is to provide a smooth airflow to the engine, approximately Mach 0.4 to 0.5. Unlike ramp or conical air inlets, it does not create oblique shock. It aims to slow the supersonic flow in a single normal shock. It has the lightest and least complex design among the geometries compared. For this reason, it is preferred in terms of production if it makes pressure recovery efficiently. To cruise at Mach 1.6 and higher Mach numbers, more than one shock wave must be created. Therefore, the preference should be air intakes with ramp entrances. Therefore, most jets designed to fly less than Mach 1.6 use a pitot inlet for lightness and simplicity reasons.

1.2.5 Aircraft selection

The McDonnell Douglas (now Boeing) T-45 Goshawk is a double seat carrier light jet trainer from BAE Systems Hawk. It is powered by a single Rolls-Royce F405-RR-401 Adour turbofan engine and provides 5,845 pounds of thrust.

2. Assistant Software

2.1 CATIA (Computer Aided Three-Dimensional Interactive Application) (Computer Aided Three-Dimensional Interactive Application) is a professional CAD/CAM based software produced by the French company Dassault Systèmes. It is used a lot, especially in the automotive sector, aircraft production and other simulation sectors. I used CATIA shape modules to draw the aircraft geometry. Sketch tracer part was used to align the images. Imagine and Shape part was used to create three-dimensional geometry.

2.2 Ansys SpaceClaim is an application that provides 3D modeling. It can perform various operations in a practical way, such as design or modelling, repairing exported CAD files, cleaning details, or editing the entire model. I used SpaceClaim to edit the geometry I drew in CATIA and to create the computational domain. At the same time, I gave my boundary conditions on SpaceClaim.

2.3 Ansys Fluent is used for editing and meshing design geometries by using CFD method. Fluent is a proven commercial software for flow analysis. The selected flight conditions are subsonic speeds. This means that the flow is compressible and turbulent. Therefore, flow dynamic modeling will be done with Reynolds-averaged Navier-Stokes's equations. The K-omega SST model was chosen because of the search for the appropriate turbulence model. The CAD drawings of the geometries were drawn with CATIA and arranged in SpaceClaim and separated into finite elements using Ansys Mesh software and transferred to the Fluent environment.

2.4 SU^2 software consists of several C++ modules. Although some modules, such as SU2_CFD, can be run alone, the real strength of the SU2 solver is that these modules can work together to perform complex tasks such as design optimization and mesh optimization. These modules are designed to perform as many different tasks as possible. The SU2 was used to simulate the project and to create different flight parameters. Boundary conditions were calculated and established for total conditioning in SU2.

2.5 Paraview is used to visualize the results of analysis. All comparison figures are in Results section.

2.6 Pointwise is used give boundary markers and check the geometry before visualizing it. Some regulations made by using Pointwise.

2.7 MS Excel is used to organize and read data in a systematic way. Tables and calculations were made using MS excel.

3. Flight Conditions

Flight condition for an aircraft can be divided into three. Take-off condition is the first part of the flight. The longest part of a jet trainer's mission phase is the cruise flight condition. Landing is the final part of the flight. In this graduation report, climb condition and cruise condition performance of the aircraft was simulated and compared according to their drag forces effects on general performance of the aircraft.

The conditions at the boundary of the domain need to be set such as inlet velocities, outlets, and wall attributes. Flight conditions are changing with Mach number, altitude, velocity, angle of attack, air density etc. Also, flight conditions have their different situations for mass flow rates. Normal design parameters have changed, and effects of air drawn by engine is observed for calculating drag force. Drag force is the main factor that we are monitoring for flight conditions.

A literature review was performed for this study and experimental studies on Y-shaped air intakes were searched. As a result of the research, for the test point DP3537 in AGARD's (The Advisory Group for Aerospace Research and Development) report named Air Intakes for High-Speed Vehicle was selected [4]. This experimental study was carried out on a subsonic air intake Model 2129 (M2129) manufactured by Royal Aircraft Establishment (RAE). According to this report my first Flight condition that is Climb arranged depends on test case 3.2 (DP3537).

3.1 Climb Condition

Climb condition has three different situations as mass flow rates. First situation is that if the engine could not draw any air. Second one is about normal flight conditions directly taken from test case 3.2 (DP3537) [4]. The last situation is a made condition and show that intake takes too much air because the beginning pressure of air intake is very low and force the engine to take more air.

SU2 configuration file allows to change in boundary conditions. All calculated values are given in this section. Compressible free-stream definition part initiates the solution. In this section, angle of attack value is given as 2^{o}. There is no side-slip angle for this analysis.

MARKER_HEATFLUX option defined as a wall with a prescribed constant heat-flux. If there is no heat-flux, it shows that it is a solid wall.

3.1.1 Closed Air Intake

This condition is about that if the engine could not draw any air. To make this condition possible, I made changes on boundary conditions. INTAKE boundary condition changed as WALL boundary condition by making it MARKER_HEATFLUX on configuration file. It means that there is no pressure effect on it.

3.1.2 Normal Flight Condition

Normal flight conditions directly taken from test case 3.2 (DP3537) [4]. This situation is a low subsonic speed, and the aircraft has flight condition climb. The altitude is 3800 ft (1158 m) at Mach 0.21 with AoA = 5°. At this condition Freestream values are as follows. Air density is 1.17634 kg/m3 and air kinematic viscosity is 14.82e-6 m2/s. Experimental data shows us that Total Pressure and Total Temperature are 101133.4 Pa and 292.996 K, respectively. Static temperature is 290.43833 K. Freestream velocity is 71.738325 m/s. About intake, following experimental data have attained by test point (DP3537). Mach 0.304 and static temperature is calculated as 287.6827 K. The velocity of air on the intake is 103.35594 m/s. Static pressure is 94855.102 Pa. According to these data Mass flow rate is calculated as 29.25 kg/s.

Table 3.1. Flight Condition: Climb-Normal Flight Conditions.

FREESTREAM-INLET			INTAKE
Altitude	Mach		Mach
3800 ft – 1158 m	0.21		0.304
T total (K)	T static (K)		T static (K)
292.996	290.44		287.68
Kinematic Viscosity (m2/s)	Velocity (m/s)		Velocity (m/s)
14.82e-6	71.74		103.356
Reynolds number	P total (Pa)		P total (Pa)
4840756	101133.4		101134.51
	P_0/P_s =1.0312		*P_0/P_s*=1.0662
Pressure at sea level (Pa)	P static (Pa)		P static (Pa)
112589.93	98073.5		94855.102
Angle of Attack (degree)	Air Density (kg/m3)	Mass flow rate (kg/s)	Air Density (kg/m3)
5	1,17634	29.25	1,14865

3.1.3 Too Open-Air Intake

Situation-3 concludes that intake takes too much air. The situation becomes valid after making intake Mach number is equal to 0.7. For this Mach number velocity will increase and the ratio of total pressure to static pressure is going to be 1.3871. Static pressure at the intake will be 72910.76 Pa. This pressure is low compared to normal situation and cause more air will be taken by the engine. In situation 3, 25.65% lower pressure was applied at the air intake compared to the normal flight condition design parameters.

Table 3.2. Flight Condition: Climb-Too open Air-Intake

FREESTREAM-INLET			INTAKE
Altitude	Mach		Mach
3800 ft - 1158 m	0.21		0.7
T total (K)	T static (K)		T static (K)
292.996	290.44		287.68
Kinematic Viscosity (m2/s)	Velocity (m/s)		Velocity (m/s)
14.82e-6	71.74		237.99
Reynolds number	P total (Pa)		P total (Pa)
4840756	101133.4		101134.51
	P_0/P_s=1.0312		P_0/P_s=1.3871
Pressure at sea level (Pa)	P static (Pa)		P static (Pa)
112589.93	98073.5		72910.76
Angle of Attack (degree)	Air Density (kg/m3)	Mass flow rate (kg/s)	Air Density (kg/m3)
5	1.17634	51.78	0.88292

In this condition, we see that the free-stream values do not change. On the other hand, intake values are changing according to Mach number. Static temperature of air-intake does not change between situation-2 and situation-3. Total temperature of intakes remains constant among these situations.

The ratio of stagnation(total) pressure to static pressure and the ratio of stagnation(total) temperature to static temperature depend on Mach number.

Finally, important change in mass flow rates. As expected, mass flow rate of too open air-intake is 51.78 kg/s and that is almost two times more than situation-2.

3.2 Cruise - 1 Condition

The cruise flight condition is the flight condition in which a jet trainer spends the most time. This situation is modeled in two ways. The first case, the Cruise-1 condition, is examined for three different air intake configurations, and these are the air intake closed condition, normal flight conditions, and finally, the air intake draws more air than normal flight conditions.

SU2 configuration file allows to change in boundary conditions. All calculated values are given in this section. Compressible free-stream definition part initiates the solution. In this section, angle of attack value is given as 5º. There is no side-slip angle for this analysis.

3.2.1 Closed Air Intake

This flight condition occurs when the air intake is completely closed. In this case, the engine cannot get air and the air intake is defined as a wall. The pressure value that should be given in the air intake is not given for this condition and the intake is defined as if it is a wall and only the free-stream values are entered as the boundary condition.

INTAKE boundary condition changed as WALL boundary condition by making it MARKER_HEATFLUX on configuration file. It means that there is no pressure effect on it.

3.2.2 Normal Flight Conditions

The normal flight condition parameters given for the Cruise-1 flight condition are the values obtained for the design geometry and recorded by this aircraft at the given flight altitude. The values given in this case can be summarized as follows. Mach number is entered as 0.4 for flight altitude 22300 ft - 6797 m. Static and total temperature values were 217.376 K and 224.332 K. The pressure value at sea level, which is normally 101325 Pa, was taken as 112589.93 Pa and the static pressure was calculated because instead of using standard values for the given flight condition, data from the test points were used. While our velocity value was measured as 132.924 m/s, the density of the air was determined as 0.56259 kg/m3.

The parameters entered for the air intake are as follows. Mach number was 0.47 and Static pressure and Static temperature values were 26252.61 Pa and 215.33 K. The air flow transmitted to the engine at the air intake was measured as 14,606 kg/s.

Calculations for cruise flight conditions are not taken with reference to the Reynolds

number. It should be noted here that the calculations were made considering the given temperature and density values. For this reason, Kinematic viscosity value and Reynolds number were not calculated.

Table 3.3. Flight Condition: Cruise-1 -Normal Flight Conditions.

FREESTREAM-INLET			INTAKE
Altitude	Mach		Mach
22300 ft - 6797 m	0.4		0.47
T total (K)	T static (K)		T static (K)
224.332	217.376		215.33
Kinematic Viscosity (m2/s)	Velocity (m/s)		Velocity (m/s)
X	132.924		139.57
Reynolds number	P total (Pa)		P total (Pa)
X	30307.76		30268.92
	P_0/P_s=1.1166		P_0/P_s=1.1667
Pressure at sea level (Pa)	P static (Pa)		P static (Pa)
112589.93	27142.9		26252.61
Angle of Attack (degree)	Air Density (kg/m3)	Mass flow rate (kg/s)	Air Density (kg/m3)
2	0.56259	14.606	0.42472

*X means that the calculations do not depend on the Reynolds number.

3.2.3 Too Open-Air Intake

In too open-air intake conditions, the Mach number for cruise-1 condition was observed as 0.65 in the air intake, which increased the speed of the engine compartment of the aircraft to 191.192 m/s. In this case, the calculated values for the air intake are as follows. Static temperature value was 215.33 K. Static and total pressure values were 20180.74 Pa and 26806.08 Pa and the ratio of total pressure to static pressure is going to be 1.3283. Air Density at this condition is 0.32649 kg/m3. As expected, the amount of air passing from the air intake to the engine increased under normal conditions and was calculated as 15.38 kg/s. The parameters given for the free-stream weather conditions Inlet and Outlet are the same as for normal air conditions. It is as follows. Mach number is entered as 0.4 for flight altitude 22300 ft - 6797 m. Static and total temperature values were 217.376 K and 224.332 K. While our velocity value was measured as 132,924 m/s, the density of the air was determined as 0.56259 kg/m3.

The important parameter in these air conditions was the back pressure in the air intake. It has entered approximately 25% less than the design values and it is aimed that the engine takes more air.

Table 3.4. Flight Condition: Cruise-1 -Too open Air-Intake

FREESTREAM-INLET			INTAKE
Altitude	Mach		Mach
22300 ft - 6797 m	0,4		0.65
T total (K)	T static (K)		T static (K)
224,332	217.376		215.33
Kinematic Viscosity (m2/s)	Velocity (m/s)		Velocity (m/s)
X	132,924		191.192
Reynolds number	P total (Pa)		P total (Pa)
X	30307,76		26806.08
	P_0/P_s=1.1166		P_0/P_s=1.3283
Pressure at sea level (Pa)	P static (Pa)		P static (Pa)
112589.93	27142.9		20180.74
Angle of Attack (degree)	Air Density (kg/m3)	Mass flow rate (kg/s)	Air Density (kg/m3)
2	0.56259	15.38	0.32649

*X means that the calculations do not depend on the Reynolds number.

3.3 Cruise – 2 Condition

The second case, Cruise-2 condition is examined for three different air intake configurations, and these are the air intake closed condition, normal flight conditions, and finally, the air intake draws more air than normal flight conditions. The importance of Cruise-2 condition is that angle of attack is zero and velocity difference between free-stream values and air intake is almost same. The aircraft will not have much difficulty in this condition.

3.3.1 Closed Air Intake

This flight condition occurs when the air intake is completely closed. In this case, the engine cannot take in air and the air inlet is defined as a wall. The pressure value specified at the air inlet is not specified in this condition, the inlet is defined like a wall, and only the free-stream values are entered as a boundary condition.

3.3.2 Normal Flight Conditions

The fluid velocity for the analysis was set to 97.0248 m/s as this was the target cruising speed of the aircraft in the conceptual study. The flow was directed to be parallel to the x-axis and in the opposite direction of it.

The fluid properties used for the analysis were the reference article properties for air. The values given in this case can be summarized as follows. Mach number is entered as 0.32 for flight altitude 30000 ft - 9144 m. Static and total temperature values were 228.8 K and 233.4904 K. The pressure value at sea level, which is normally 101325 Pa, was taken as 112589.93 Pa and the static pressure was calculated because instead of using standard values for the given flight condition, data from the test points were used. While our velocity value was measured as 97.0248 m/s, the density of the air was determined as 0.35276 kg/m3.

Table 3.5. Flight Condition: Cruise-1 -Normal Flight Conditions.

FREESTREAM-INLET			INTAKE
Altitude	Mach		Mach
30000 ft - 9144 m	0.32		0.322
T total (K)	T static (K)		T static (K)
233.4904	228.8		226.64
Kinematic Viscosity (m2/s)	Velocity (m/s)		Velocity (m/s)
X	97.0248		97.0346
Reynolds number	P total (Pa)		P total (Pa)
X	24871.4277		24078.051
	P_0/P_s=1.0735		P_0/P_s=1.0745
Pressure at sea level (Pa)	P static (Pa)		P static (Pa)
112589.93	23168.54		22408.61
Angle of Attack (degree)	Air Density (kg/m3)	Mass flow rate (kg/s)	Air Density (kg/m3)
0	0.35276	8.235	0.34444

*X means that the calculations do not depend on the Reynolds number.

3.3.3 Too Open-Air Intake

Too open-air intake means that the back pressure of air intake will be decreased by 25% according to free-stream pressure value and this will affect the air drawn by the engine. The engine will take more air than normal flight which causes a change in the pressure

distribution of the intake. This will change the Mach number and velocity as 0.45 and 135.7956 m/s, respectively.

Table 3.6. Flight Condition: Cruise-2 -Too open Air-Intake

FREESTREAM-INLET			INTAKE
Altitude	Mach		Mach
30000 ft - 9144 m	0.32		0.45
T total (K)	T static (K)		T static (K)
233.4904	228.8		226.64
Kinematic Viscosity (m2/s)	Velocity (m/s)		Velocity (m/s)
X	97,0248		135.7956
Reynolds number	P total (Pa)		P total (Pa)
X	24871.4277		19794.17
	P_0/P_s=1.0735		*P_0/P_s*=1.1491
Pressure at sea level (Pa)	P static (Pa)		P static (Pa)
112589.93	23168.54		17225.8
Angle of Attack (degree)	Air Density (kg/m3)	Mass flow rate (kg/s)	Air Density (kg/m3)
0	0.35276	31.625	0.264777

*X means that the calculations do not depend on the Reynolds number.

4. Geometry

Firstly, I determine the type of aircraft. Subsonic or supersonic aircraft were available on the table. Then my supervisor and I agree on subsonic aircraft. After that, a literature review was conducted to identify the aircraft. Jet trainers using subsonic pitot type air intakes were investigated. To determine the geometry, air intake configurations were examined by conducting a study on jet trainers. Among the configurations, the commonly used Y-shaped flush type was chosen. At the same time this intake is used for HURJET which is a military training aircraft that will be designed, developed, and produced as a jet powered training and air support aircraft by Turkish Aerospace Industries Inc. In this study, flight conditions and diffuser dimensions were determined according to the characteristics of the T-45 Goshawk aircraft. The T-45 Goshawk aircraft is an advanced training and light fighter aircraft developed by McDonnell Douglas (now Boeing). The aircraft is powered by a single Rolls-Royce F405-RR-401 Adour turbofan engine, providing 5,845 pounds of thrust.

4.1 Model

A 3D model of the aircraft is available, as well as all the relevant measurements of the aircraft geometry (see Figure 4.1 and 4.2).

The T-45 Goshawk is a fully carrier-capable version of jet flight trainer. Rolls-Royce provided the Adour engine to power the aircraft.

4.1.1 General characteristics

Crew: 2

Length: (11.99 m), Wingspan: (9.3917 m), Height: (4.11 m).

Maximum speed: 1,006 km/h at 8,000 ft (2,438 m) and M=0.84 at 30,000 ft (9,144 m).

Carrier launch speed: (139 mph; 224 km/h).

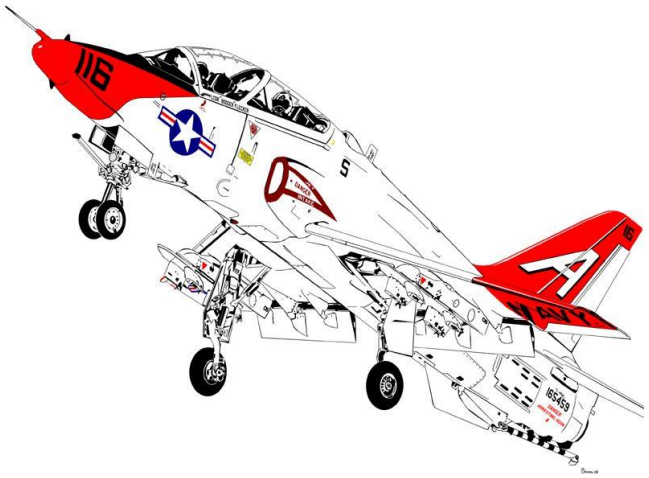

Figure 4.1. Three-dimensional view of the aircraft.

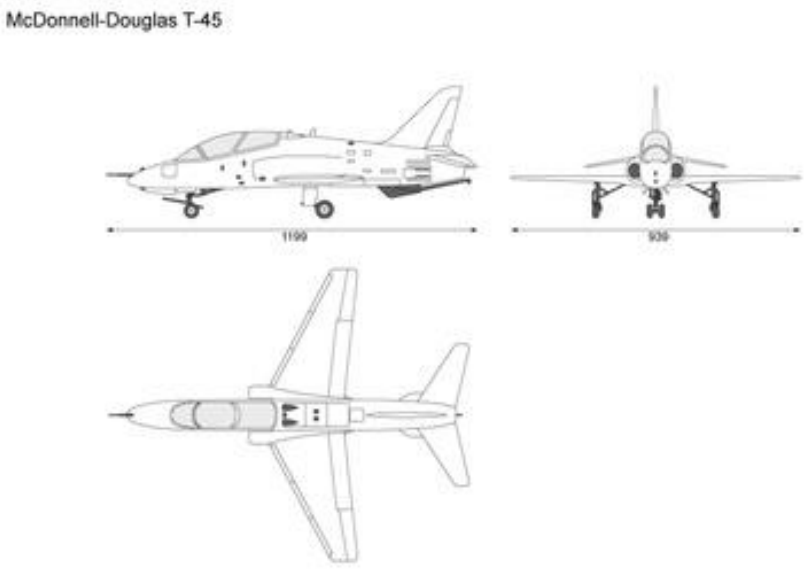

Figure 4.2. Three view drawing.

4.2 CAD Drawing

The CAD drawing was created using CATIA V5R21. CATIA's shape module is used here. Using the sketch tracer, the blueprints of the drawing were transferred to the program. The drawing was carried out using the actual dimensions of the aircraft. Geometry was created in three dimensional using CATIA's Imagine and shape module. Ansys SpaceClaim can be used to repair exported CAD file, clean details, and edit the entire model. The figures below show the stages of CAD drawing.

4.2.1 Coordinate System

The model is placed in a Cartesian coordinate system and is oriented so that the x-axis represents the aircraft's roll axis, the y-axis represents the pitch axis, and the z-axis represents the yaw axis (see Fig. 6.1).

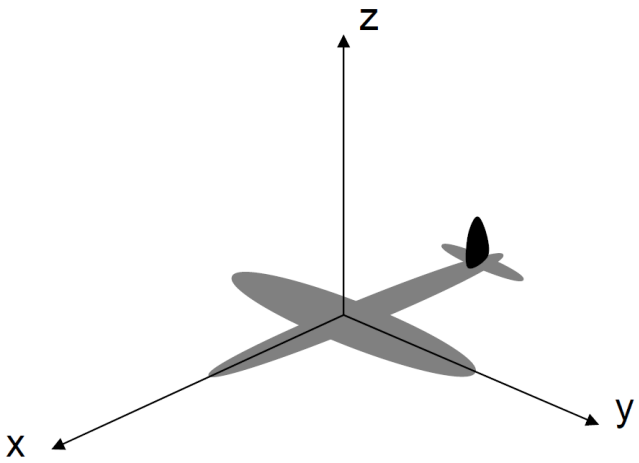

Figure 4.3. The model's orientation in relation to the Cartesian coordinate system.

4.2.2 Advantage of Symmetry

To speed up the computations and to concentrate the computer resources, advantage will be taken of the model's symmetry. Since the model and domain is symmetric around the XZ-plane, the computations only need to be carried out on one half of the domain, since the other half will yield the same, but mirrored, results. This way, the number of elements needed can be halved and thus cutting computation time by half.

Symmetry was also used in the domain size study where the cylinder and its domain were symmetric around the XZ-plane, reducing the size of the domain to one half of its original size.

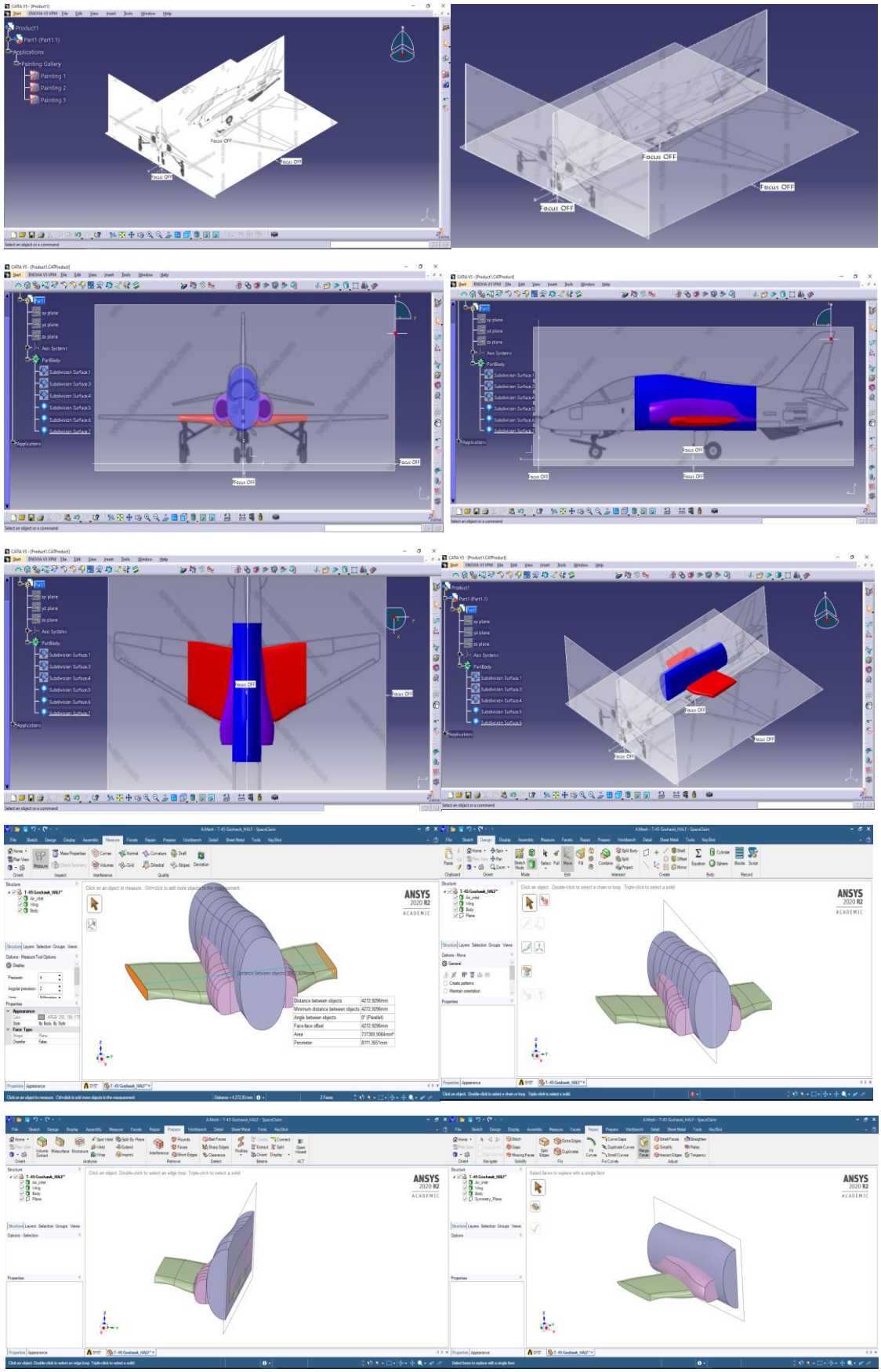

Figure 4.4. CAD Drawing stages.

4.2.2 Domain properties

Several different shapes were considered for the computational domain in this study. At first a spherical domain seemed like the best solution since the distance from the model to the domain boundaries would be close to equal in all directions, meaning that the volume of the domain could be kept to a minimum. This idea was dropped in favor for a cylindrical domain which was better suited for modelling and applying boundary conditions, although there would be some wasted space in the corners that would have little to no effect on the result, meaning that the computations might take a little longer than an optimal shape would.

Domain size is a complicated issue for aircraft modeling because There was very little information to be found on how large a domain was required for a study such as this one, since so many different factors come into play making each case unique. However, a rough indication was that at least 10 times the model length would be required in each direction to obtain somewhat accurate results.

Since a too large domain would waste computational resources and a too small domain would lead to inaccurate drag estimations, a study was required to determine exactly how small a domain could be used without affecting the result.

With the aircraft in the centered in the domain, it gives a domain size between ~15 m and 35 meters in each direction, roughly 8 times the aircraft length of ~2.15 m and 4.43 m.

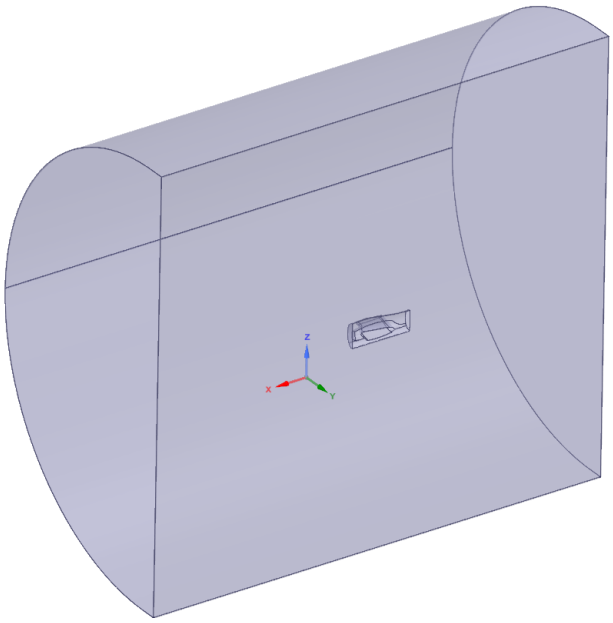

Figure 4.5. Computational Domain.

5. CFD Flow Analysis

In order to obtain the best results possible, the CFD analysis requires careful planning. The simulation itself can take several days, or even weeks, so there will be no opportunity to re-run the simulation once it has been completed. The planning of the final simulation has been broken down into smaller steps to set up the analysis.

5.1 Numerical Model

In this report, there are two simulations. First simulation is made by using Ansys Fluent which is a commercial software. Second simulation is made by using SU^2 and this software is an open source CFD software.

5.1.1 Ansys Fluent Simulation

There are several different CFD solvers available on the market. For this analysis Ansys Fluent has been chosen as this is the one available and determined to be sufficient for the analysis. The first analysis run was modeled using the CFD method. The experimental test setup is in the subsonic compressible flow region. When the Reynolds calculation was made with the experimental conditions, it was calculated that the flow was in the compressible and turbulent region. Therefore, flow dynamic modeling will be done with Reynolds-Averaged Navier-Stokes's equations. As a result of the search for the appropriate turbulence model, it was determined that the k-omega (ω) SST model gave the closest results to the experimental data, as Menzies Ryan DD stated in his validation on RAE M2129 with various turbulence models in his study called Investigation of S-Shaped Intake Aerodynamics Using Computational Fluid Dynamics [5]. The k - ω SST is a two-equation eddy viscosity model. The shear stress transfer (SST) equation operates the two models in combination. While SST uses the k-ω model for calculations close to the wall and within the boundary layer, it uses the k-epsilon(ε) model for free flow regions away from the wall. Since the k-ω model is too sensitive for free flow modeling, the K- ω SST model offers a suitable model for all flow. For this reason, the k-omega SST model was chosen as the turbulence model. CAD drawings of the geometries were created with the CATIA V5R21 program, separated into finite elements and transferred to the Fluent environment.

5.1.2 SU^2 Simulation

The second analysis run was modeled using the SU^2 software. This software does not use graphical user interface and needs to put all parameters on configuration file.

In this study, analyzes were performed with three different flight conditions (angle of attack) and Spalart–Allmaras turbulence model. Analyzes were performed with the SU2 open-source solver. Solver type "RANS (Reynolds-averaged Navier-Stokes)" is selected. This solvent together with JST (Jameson-Schmidt-Turkel) solver gives accurate results in boundary layer analysis. The JST centripetal scheme tries to get more precise results using quadratic equations. DIMENSIONAL was chosen as the compressible flow nondimensionalization method. In this way, the nondimensionalization process was done manually. STANDARD_AIR was used as the gas model. The Viscosity model was chosen as SUTHERLAND and the CONSTANT_PRANDTL thermal conductivity model was used. Our numerical method is GREEN_GAUSS. The flow CFL number was set at 0.8.

5.1.2.1 Convergence Criteria

The Criteria for which the simulation can be regarded as converged needs to be determined. It was started for 100000 iterations but took about 20000 iterations, varying with each analysis. To control the series convergence set at 1E-6. Convergence criteria field is DRAG. Start convergence criteria at iteration number at 10 and the number of elements to apply the criteria is 100.

5.1.2.2 Post Processing

The simulation results will give the sums of the forces acting on the model. Through this, the drag coefficient C_D can be obtained. Drag force and the amount of lift created by the wing are calculated by applying integration on the model.

In the Post Process part, the results were visualized by using the Paraview software.

Post processing includes the comparisons of Mach number, Pressure, Drag, Lift, Momentum, and Velocity.

From the obtained Mach number, pressure, and momentum graphs, it is seen that the open-source solver SU2 predicts the flow schemes well in low velocity regimes. It is thought that the applied effect geometry solution mesh structure study is effective in estimating SU2 correctly.

5.2 Mesh

The external flow computational domain was created by using SpaceClaim. Domain size generated according to SU2 tutorials (Turbulent_ONERAM6) [7].

The geometry mesh was created using Ansys' mesh interface. The important element in mesh creation is to create the geometry with the minimum number of elements to solve the analyzes in the least amount of time. The mesh structure was created by considering the general quality criteria and the boundary conditions of all surfaces were checked at this stage.

The boundary layer is the region where the velocity gradient is very high, and the viscosity effects are dominant. This region must be divided into much smaller elements than normal geometry. Since the flow is completely turbulent, it reduces the target element size in the boundary layer mesh to the smallest eddy size. The boundary layer mesh is modeled with layers stacked with a growth rate and first layer thickness in the Inflation command in the Ansys Mesh tool. To model the boundary layer velocity distribution in the most accurate way, boundary layer mesh was applied to the entire wet area with the Inflation option in Ansys.

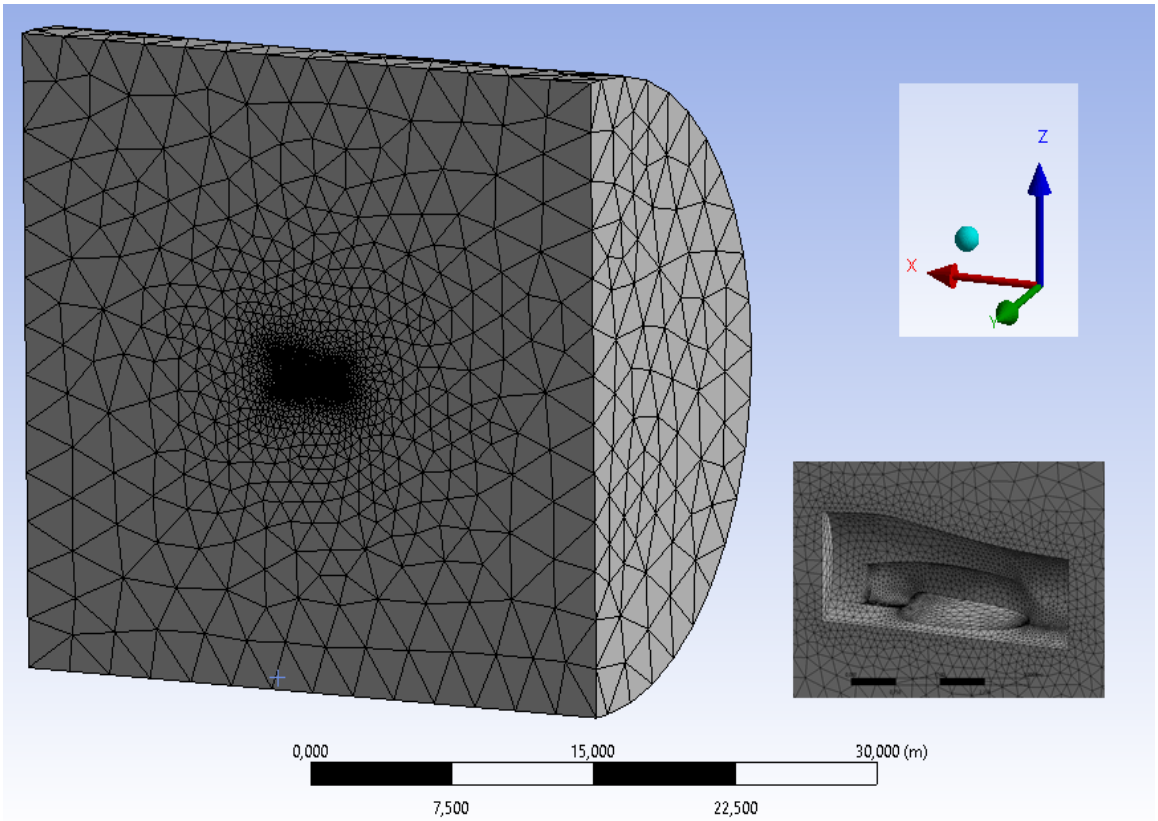

Figure 5.1. Mesh structure of SU2 analysis

SU2 analysis was performed without considering boundary layer conditions. The important parameter here was to observe the correct distribution of pressure gradients. Shear stresses and viscous effects are ignored.

Table 5.1. Fluent Mesh Criteria

Physics preference	CFD
Solver preference	Fluent
Element order	Linear
Element size	0.3 m
Curvature normal angle	8°
Capture proximity	No
Smoothing	High
Skewness (max)	0.83956
Orthogonal quality (min)	0.15229
Inflation	Yes
Inflation option	First layer thickness
First layer height	0.0032 m
Maximum layers	7
Growth rate	1.2
Number of nodes	111447
Number of elements	420941

Table 5.2. SU2 Mesh Criteria

Physics preference	CFD
Solver preference	Fluent
Element order	Linear
Element size	2.4985 m
Curvature normal angle	18°
Capture proximity	No
Smoothing	Medium
Skewness (max)	0.81505
Orthogonal quality (min)	0.18495
Inflation	None
Inflation option	Smooth transition
First layer height	X
Maximum layers	5
Growth rate	1.2
Number of nodes	32110
Number of elements	176064

5.3 Design Numeric Model

The setting of the design analyzes are made differently for Ansys analysis and SU2 analysis. Ansys analysis was simulated with Fluent software using the k-omega SST turbulence model. Boundary layer calculations have been made and geometry meshes have been obtained in a way that will not increase the solution time in the design geometry and can get results close to the real solution. Figure 5.1 shows the mesh structure of the design geometry.

5.3.1 The Computational Domain

The appropriate size and shape of the computational domain, also referred to as control volume, and the best placement of the model in the domain, needs to be determined. A domain too large will make the simulation unnecessarily large and waste computational resources, however a domain too small will lower the accuracy of the results. The properties of the domain such as temperature, pressure and fluid properties need to be chosen.

5.3.2 Discretization of the Domain

Since CFD utilizes numerical solutions, the domain needs to be discretized or meshed as it is more commonly referred to. The mesh will have to be refined in areas with high gradients for example close to the surface around the aircraft model.
As the boundary condition, the wing and the fuselage of the aircraft were accepted as the wall, and the solution area in which it was located was determined as Far Field. In the wall condition, the velocity on the surface is zero.

5.3.3 Boundary Conditions

The domain has 5 different types of boundaries surrounding it.

- INLET: At the inlet, the boundary condition was set to inlet marker, total temperature, total pressure, flow direction where flow direction is a unit vector. This would give a flow parallel to the longitudinal X-axis of the model.
- OUTLET: At the outlet boundary, the back pressure was set to flight condition as which condition is applied. This is the free-stream pressure as well.
- INTAKE: At the Intake boundary, the back pressure is changed according to the flight condition. This means that the air leaving the INLET boundary condition.
- SYMMETRY: Symmetry plane: Symmetry was used in the domain size study where the aircraft and its domain were symmetric around the XZ-plane, reducing the size of the domain to one half of its original size.
- FARFIELD: In the Far Field boundary condition, the boundary conditions (Mach number and free-stream conditions) given for the model are defined at infinity in free-stream conditions.
- WING: Defined as wall.
- BODY: Defined as wall.

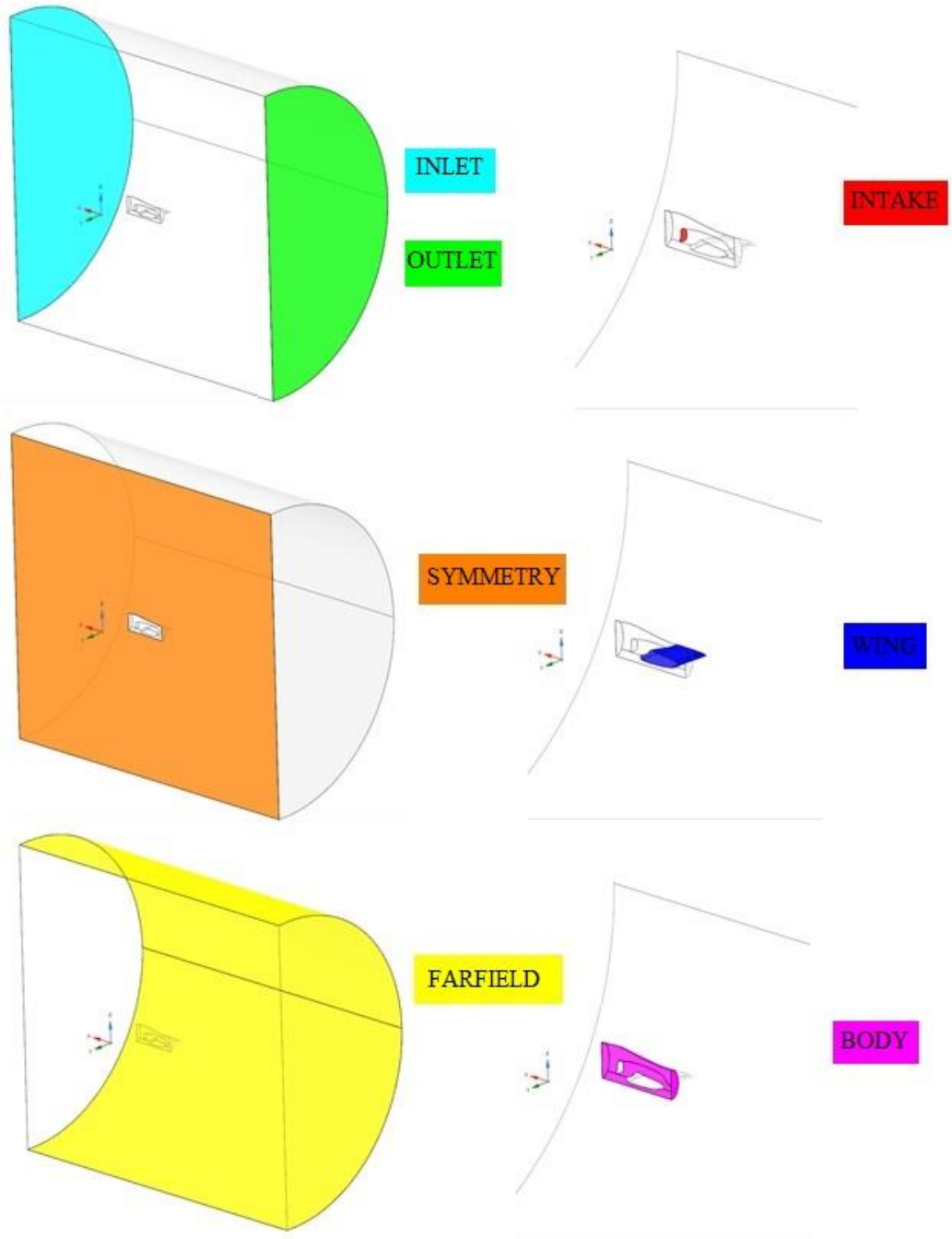

Figure 5.2. Boundary Condition Markers

Half of the geometry is modeled because the flow is symmetrical with respect to the XZ plane. As a result, a numerical model of the design geometry is created with the obtained settings. Analysis using Ansys Fluent was run for a single flight condition and the results were as predicted. Since the results for Pressure and Velocity were as expected, it helped to form an idea about the parameters before the SU2 analysis. This report does not compare the Analysis results of SU2 and Ansys Fluent.

6. Results

As a result of this study, analyzes were made for the subsonic air intake of the McDonnell Douglas T-45 Goshawk jet trainer. The drag forces and effects of the air intake were investigated depending on the amount of air drawn by the engine and flight conditions. Comparisons were made in other effects such as Mach numbers, pressure, velocity. Examining these forces and their effects with CFD methods plays an important role in the design of the air intake and the overall performance of the aircraft.

Analysis using Ansys Fluent was run for a single flight condition and the results were as predicted. Since the results for Pressure and Velocity contour were as expected, it helped to form an idea about the parameters before the SU2 analysis. This report does not compare the analysis results of SU2 and Ansys Fluent.

In this report, analyzes of the air intake of the T-45 Goshawk fighter trainer aircraft were run for three different flight conditions.

In each flight condition, analyzes were run for three different conditions. The air intake is closed, the normal flight situation given in accordance with the design parameters, and finally, the situation where more air is drawn in the air intake than the normal condition by the engine.

In this report, comparisons were made for Drag and Lift forces and the results are shown below. As expected in all the given flight conditions, the drag force was higher for the case where the air intake was closed. Different results have emerged in the comparisons made regarding the lift force. This is because the analysis is run depending on the convergence parameter drag coefficient. As a result, although the Drag coefficient converged at the end of the analysis, the Lift coefficient may not have converged yet or may have converged much earlier. In this case, it is not correct to make a comparison for the lift force according to the graphics and results obtained.

The total duration of the analyzes to be obtained because of the geometry and computational domain created lasted approximately 100 hours. With the analyzes made before but not shown as a result, this period becomes much longer.

6.1 Comparison-Flight Condition: Climb

The figure and explanations below indicate the climb condition comparisons of Mach number, Pressure distribution, drag force and lift force.

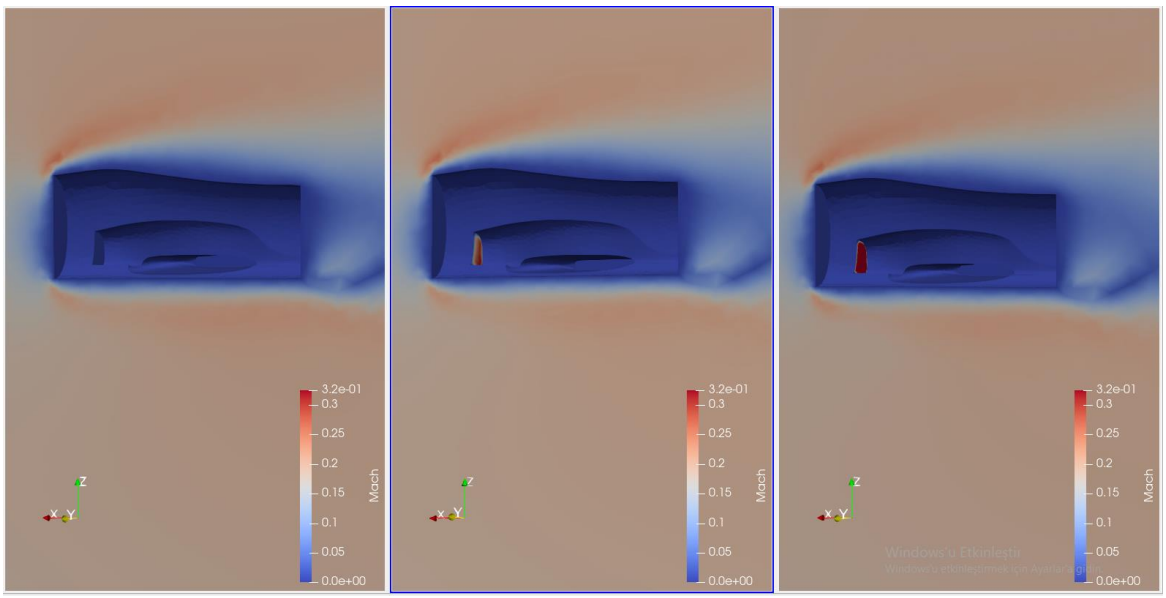

Figure 6.1. Mach Number Comparison.

As we see in the Figure 1.1, Mach number becomes zero at close air intake because of there is not air drawn by the engine. In normal flight condition, Mach number is getting increase by edge of the intake. This distribution is not identical in intake geometry because angle of attack was 5^{o} at this condition. This affects where the air will be taken by the intake surface. Third picture show us the Mach number distribution of too open-air intake. This indicates that the inlet is drawing in as much air as possible.

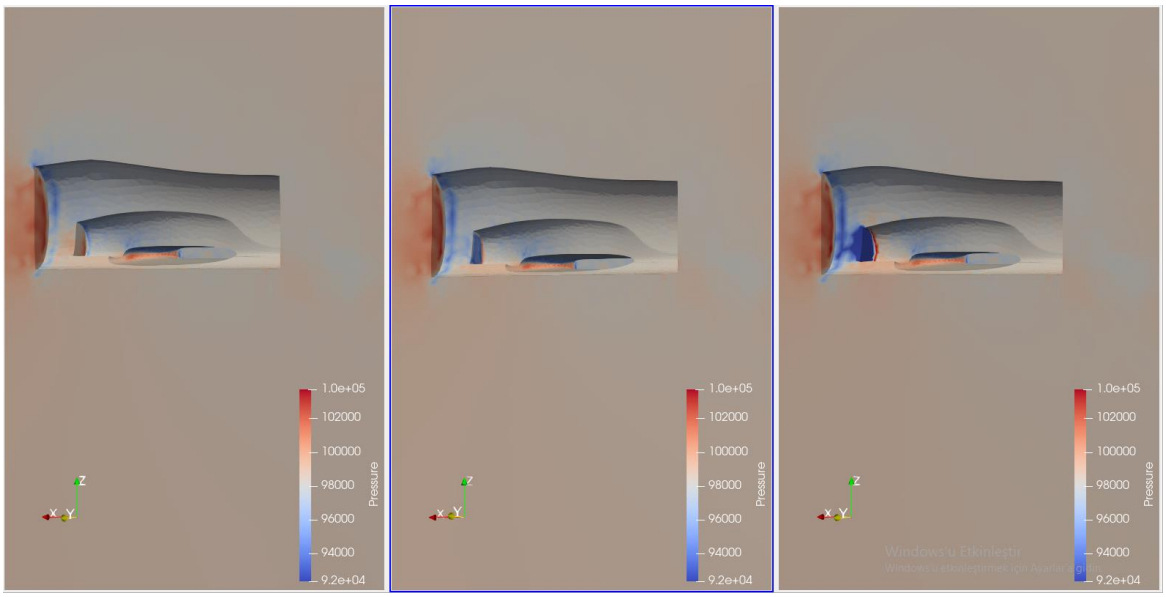

Figure 6.2. Pressure Comparison.

Figure 1.2 shows the pressure distribution and here is the third photo that draws attention. The pressure is so low that the air intake inlet surface and its surroundings have dropped to about 90 kPa. Since the front part of the plane geometry is cut in all pictures, pressure rise is seen, and it is as expected.

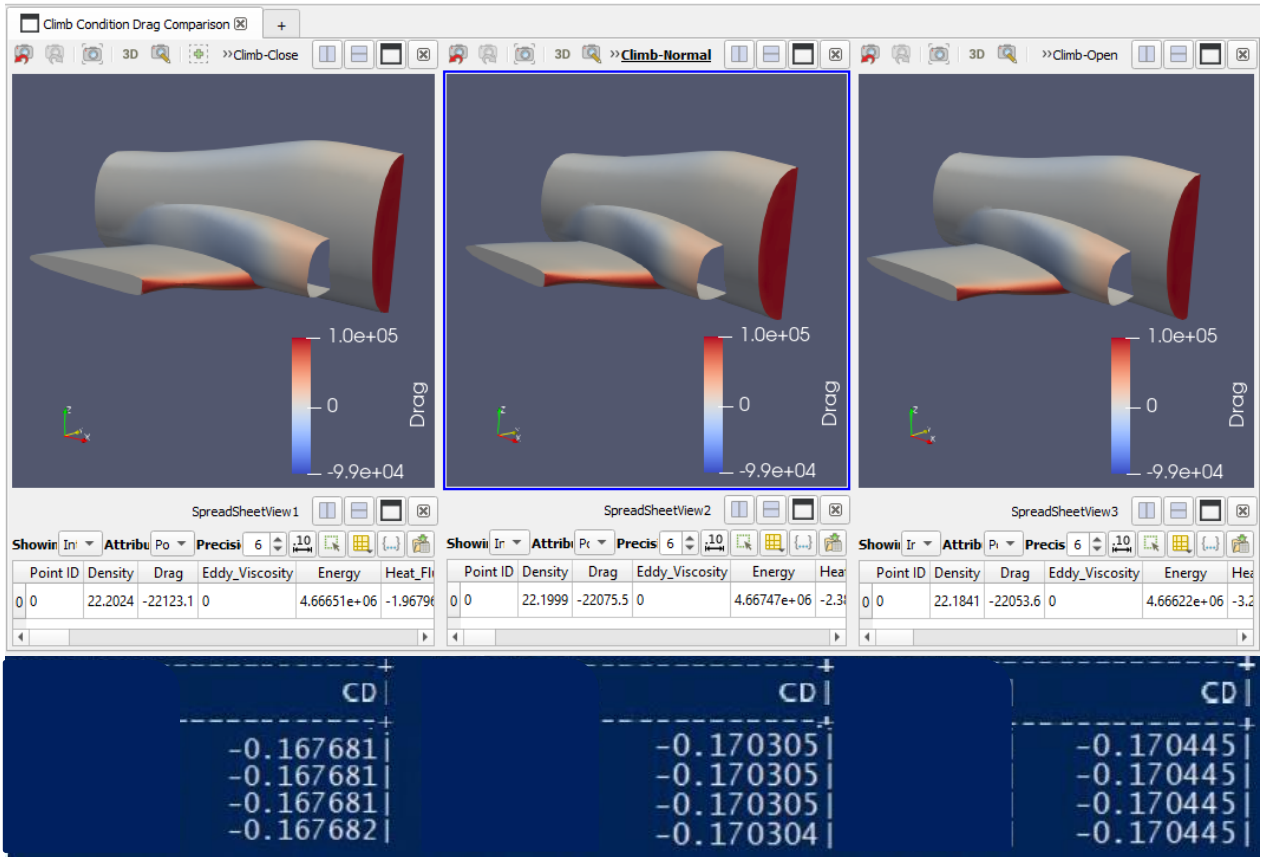

Figure 6.3. Drag Force and Drag Coefficient Comparison.

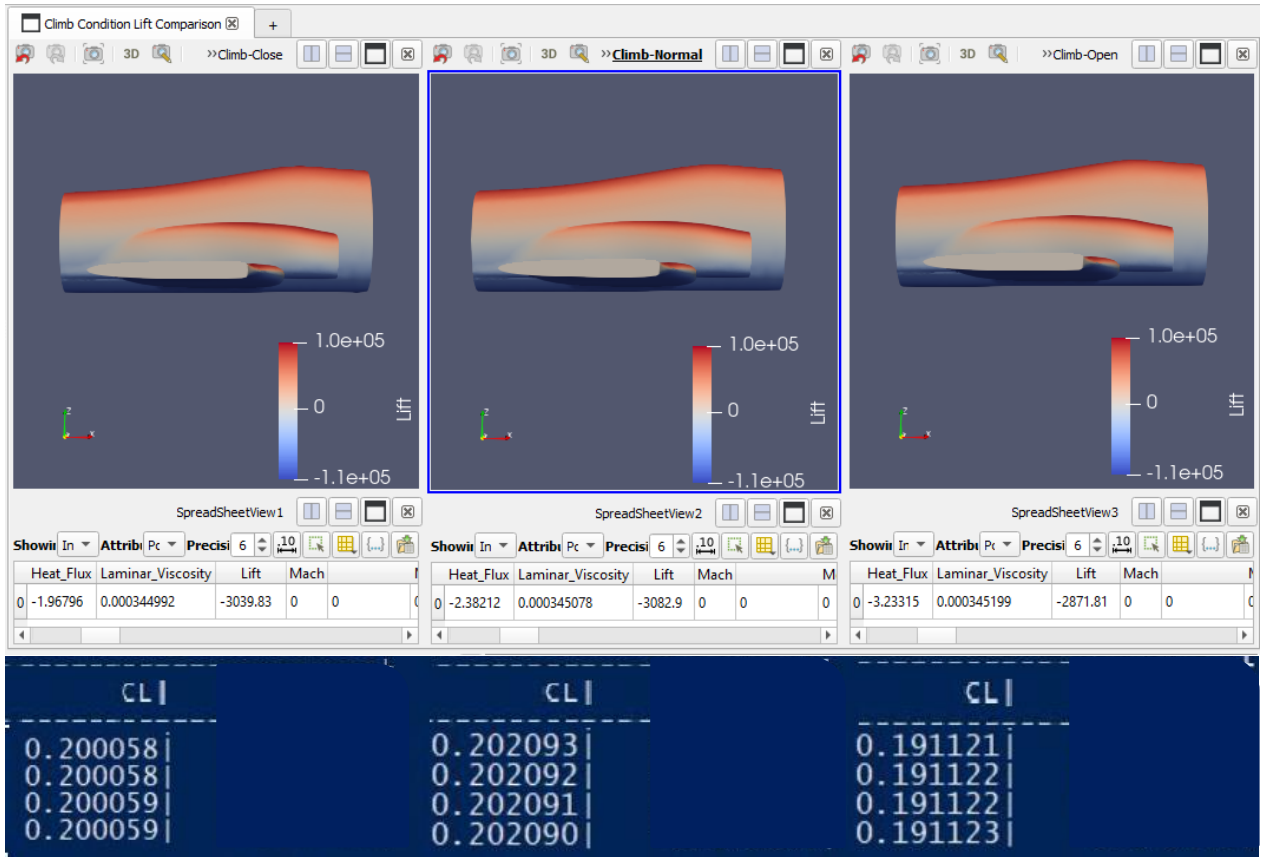

Figure 6.4. Lift Force and Lift Coefficient Comparison.

Drag, Lift Forces and Drag, Lift coefficients of Climb condition are as follows.

Close air intake:	Close air intake:
F_D=22123.1 N and C_D=0.167682	F_L=3039.83 N and C_L=0.200059
Normal air intake:	Normal air intake:
F_D=22075.5 N and C_D=0.170304	F_L=3082.9 N and C_L=0.202090
Open air intake:	Open air intake:
F_D=22053.6 N and C_D=0.170445	F_L=2871.81 N and C_L=0.191123

Firstly, although there are images, it would be difficult to comment directly on the images as the values are close to each other. Therefore, the numerical equivalents of the values were also calculated.

It can be understood from here that the drag force is greatest when the air intake is closed. This is the expected result because when it is closed, the air intake is modeled as a wall and increases the surface area. In addition, although it has the lowest drag coefficient, the given air conditions determined it to be the one with the highest drag effect. Half of the geometry is modeled. Since the air intake inlet is given to the model through the x-axis, the drag effects on the front body are positive, while the fuselage drag is negative in the invisible part of the pictures.

The following can be said about the lift force, and this will be valid for all calculations. In the solution, the convergence criterion was determined as the drag coefficient. The iteration stopped when the drag coefficient value was lower than 1e-6. When we look at the iteration results, although the drag coefficient has converged, it has been observed that the lift coefficient has not converged yet or has converged before. In the face of this result, it is not correct to comment on the lift forces because the lift coefficient, reference area, density and velocity values change.

6.2 Comparison-Flight Condition: Cruise-1

The experimental mass flow results were applied to a computational model in SU2, an existing computational fluid dynamic (CFD) program, which predicted the flow around the air-intake simulator. This information will provide a strong foundation and framework to build and expand the use of computational modeling in jet engine test simulations. To analyze the drag effects caused by air-intake, an intake simulator, a scale model of a jet engine, was operated at varying adverse operational conditions to understand which conditions how will generate drag effects.

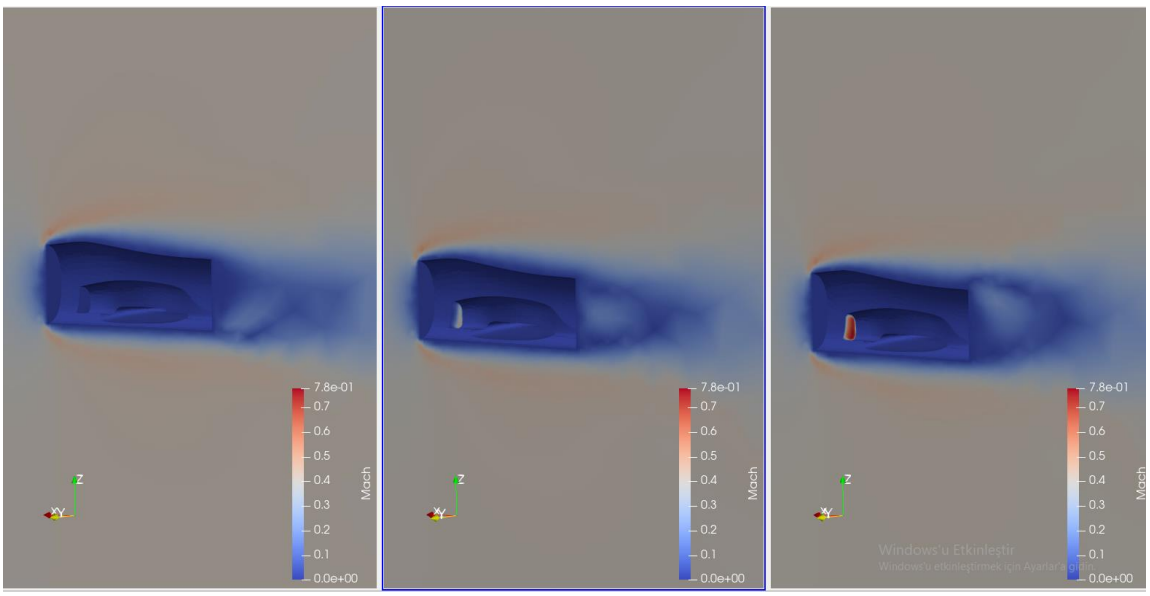

Figure 6.5. Mach Number Comparison.

The computations on the intake are carried out for Mach number ranging from zero to high subsonic speeds. At inflow, total pressure, and total temperature of 30307.76 Pa and 224.332 K are imposed. At intake exit, the back pressure was adjusted to obtain the corrected mass flow rate desired by the engine. For low subsonic Mach no, computations are also carried out at AOA= 2^{o} to evaluate cruise performance.

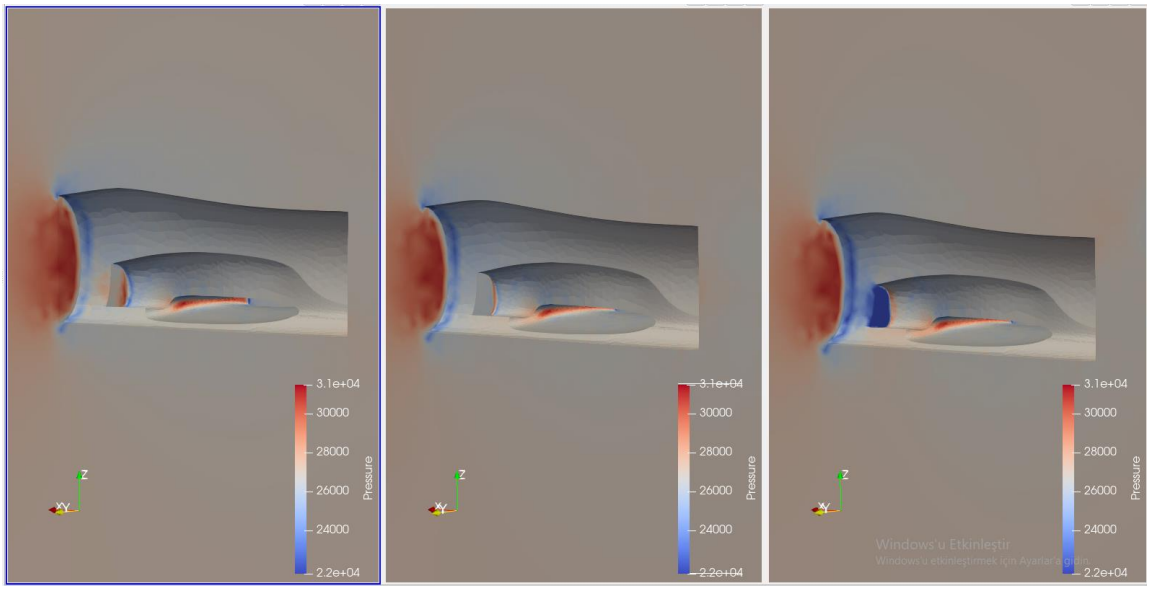

Figure 6.6. Pressure Comparison.

Figure 6.6 shows the pressure distribution and here is the third photo that draws attention. The pressure is so low that the air intake inlet surface and its surroundings have dropped to about 20 kPa. From intake geometry, pressure increase can be seen on the edge of inlet. As the front part of the plane was cut while drawing the model, pressure rise was observed.

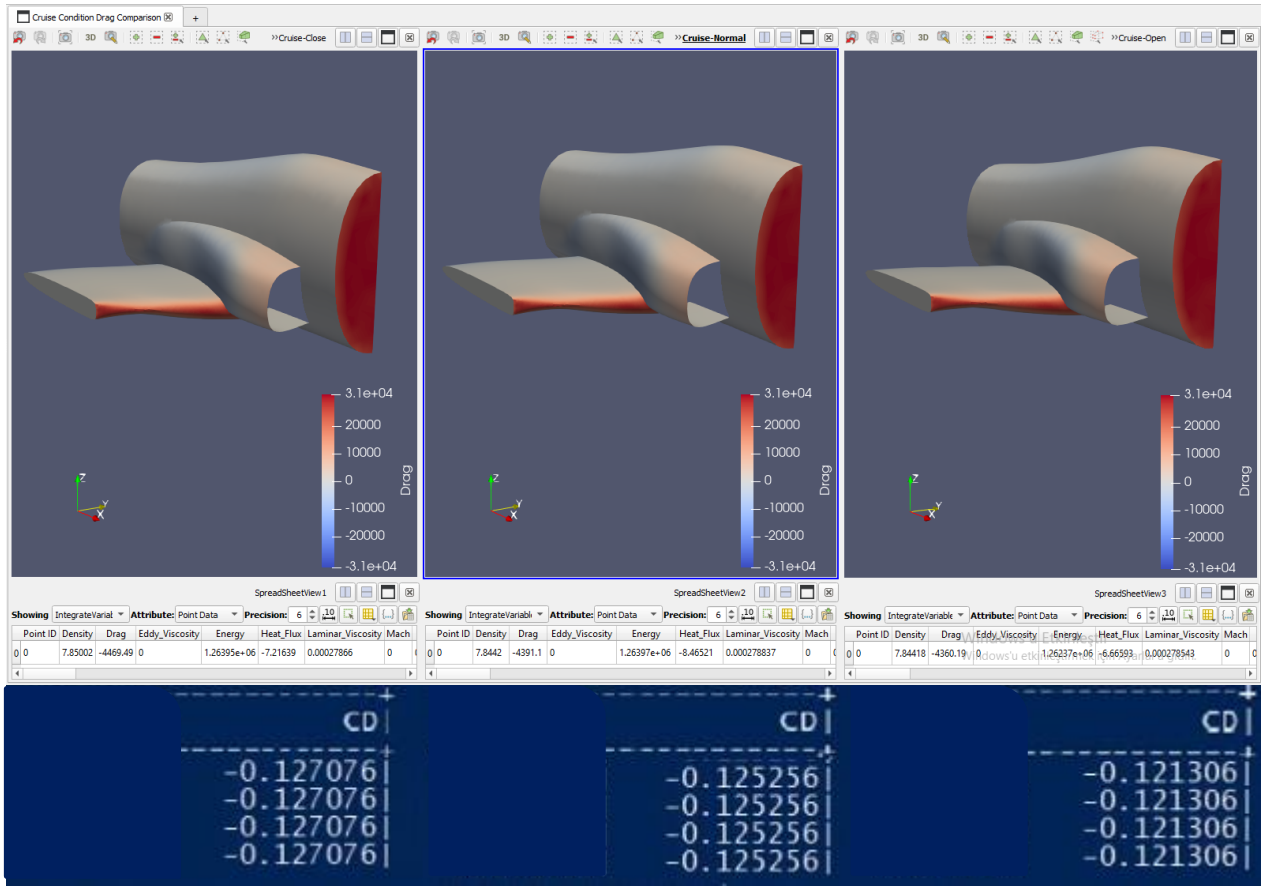

Figure 6.7. Drag Force and Drag Coefficient Comparison.

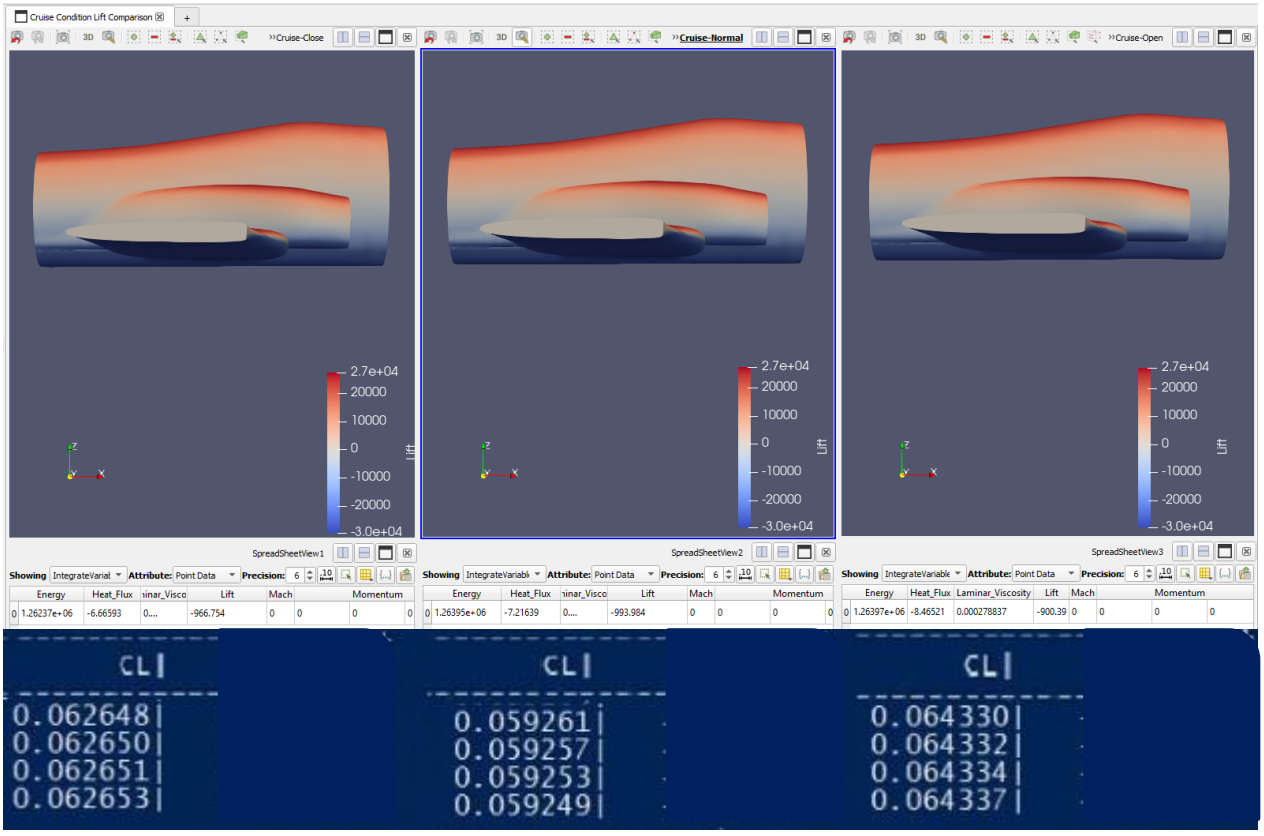

Figure 6.8. Lift Force and Lift Coefficient Comparison.

Drag, Lift Forces and Drag, Lift coefficients of Climb condition are as follows.

Close air intake:	Close air intake:
F_D=4469.49 N and C_D=0.127076	F_L=966.754 N and C_L=0.062648
Normal air intake:	Normal air intake:
F_D=4391.1 N and C_D=0.125256	F_L=993.984 N and C_L=0.059249
Open air intake:	Open air intake:
F_D=4360.19 N and C_D=0.121306	F_L=900.39 N and C_L=0.064337

Another performance parameter is the intake drag force. The lower the drag force (D), the higher the coupled thrust of the engine, so the reduction of the thrust drag force will increase the performance of the engine. D is calculated by the downstream component of the pressure and viscous forces on the lip and diffuser walls. Drag values seem sufficient. On the other hand, the precision of the analysis can be improved by increasing the number of geometries, if desired. Although the applied physical method is successful in estimating the drag coefficient, the accuracy of the numerical solution is not exact since this situation depends on the mesh criteria and convergence criteria.

Firstly, although there are images, it would be difficult to comment directly on the images as the values are close to each other. Therefore, the numerical equivalents of the values were also calculated.

It can be understood from here that the drag force is greatest when the air intake is closed. This is the expected result because when it is closed, the air intake is modeled as a wall and increases the surface area. In addition, although it has the lowest drag coefficient, the given air conditions determined it to be the one with the highest drag effect.

The following can be said about the lift force, and this will be valid for all calculations. In the solution, the convergence criterion was determined as the drag coefficient. The iteration stopped when the drag coefficient value was lower than 1e-6. When we look at the iteration results, although the drag coefficient has converged, it has been observed that the lift coefficient has not converged yet or has converged before. In the face of this result, it is not correct to comment on the lift forces because the lift coefficient, reference area, density and velocity values change.

6.3 Comparison-Flight Condition: Cruise-2

The figure and explanations below indicate the climb condition comparisons of Mach number, Pressure distribution, drag force and lift force.

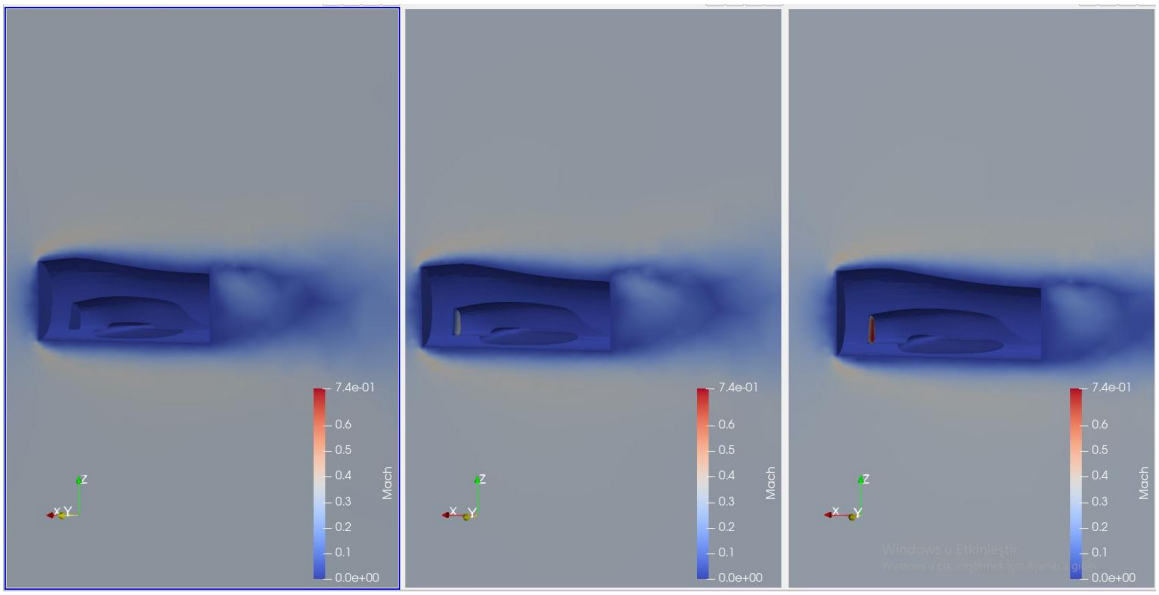

Figure 6.9. Mach Number Comparison.

The isometric view Mach number is shown in figures 6.9. The variation of Mach number due to changes in duct mass flow rate can be seen in figure 6.9.

The computations on the intake are carried out for Mach number ranging from close air-intake to too open air-intake. At intake exit, the back pressure was adjusted to obtain the corrected mass flow rate desired by the engine. The computations are also carried out at AOA= 0^{o} and Spalart-Allmaras model is used for turbulence and equations are solved by Jameson scheme. to evaluate cruise performance.

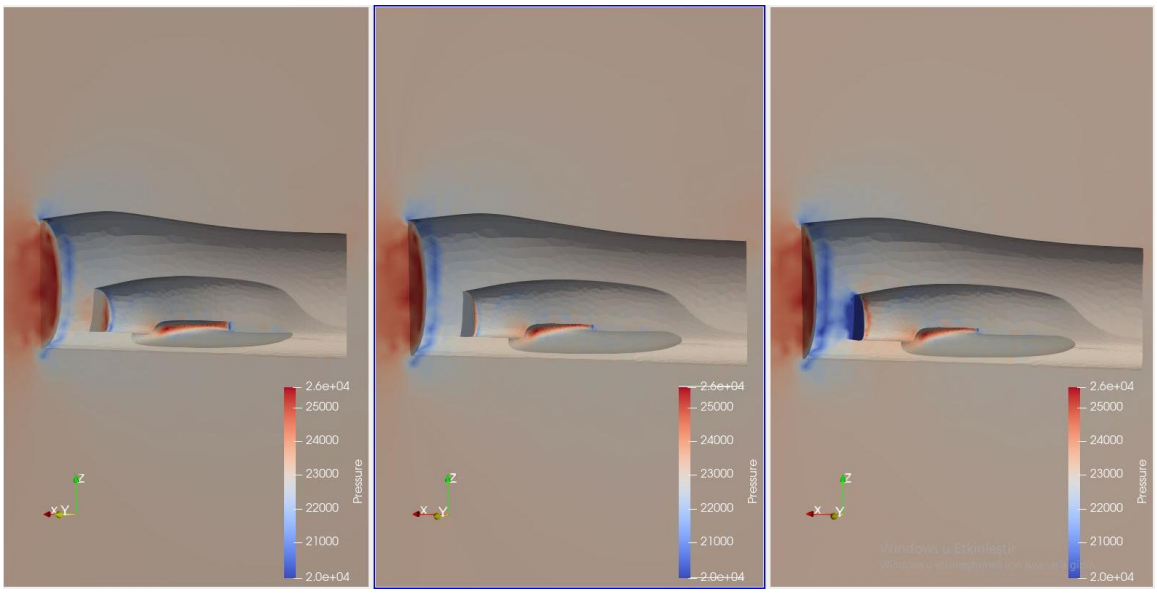

Figure 6.10. Pressure Comparison.

The isometric view pressure distribution is shown in figure 1.2. Significant total pressure loss is observed due to too open air-intake situation in third picture. From intake geometry, pressure increase can be seen on the edge of inlet.

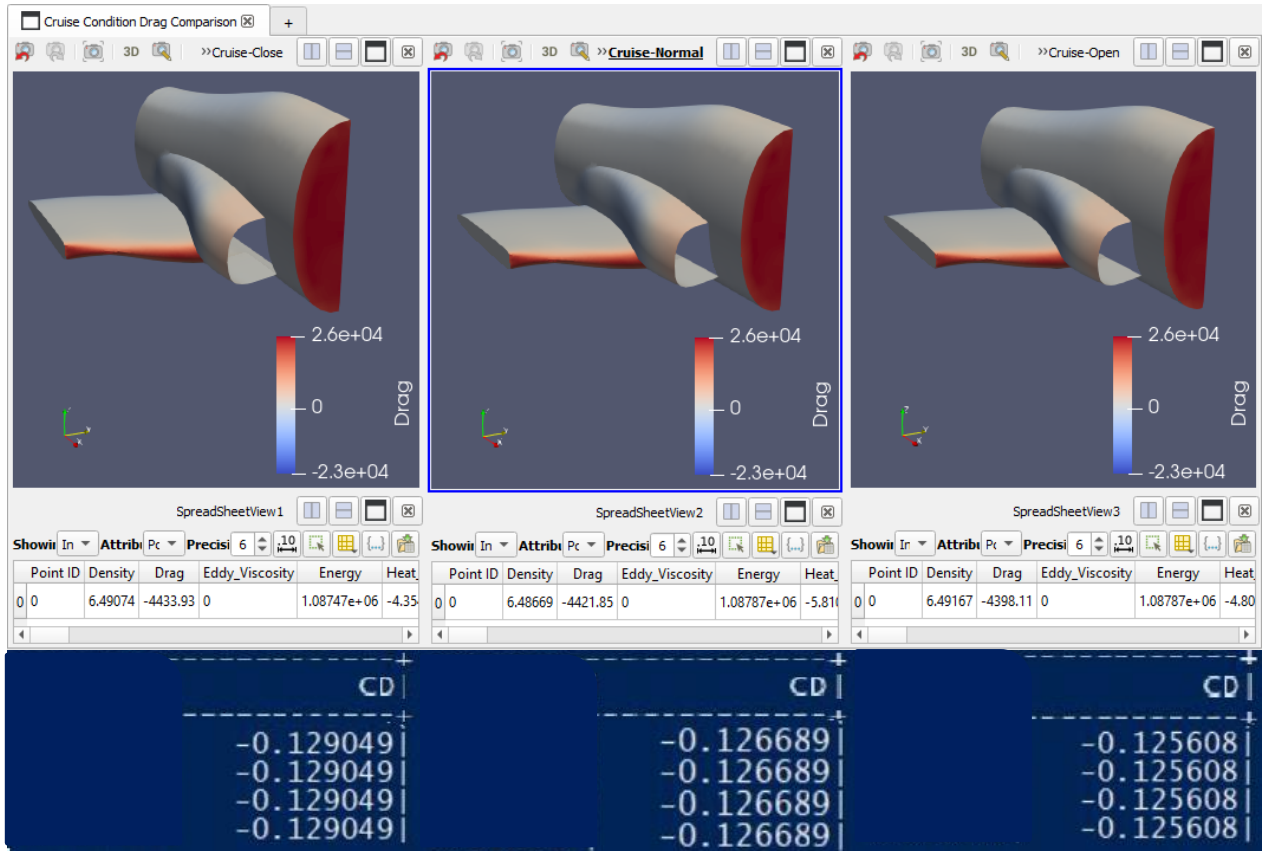

Figure 6.11. Drag Force and Drag Coefficient Comparison.

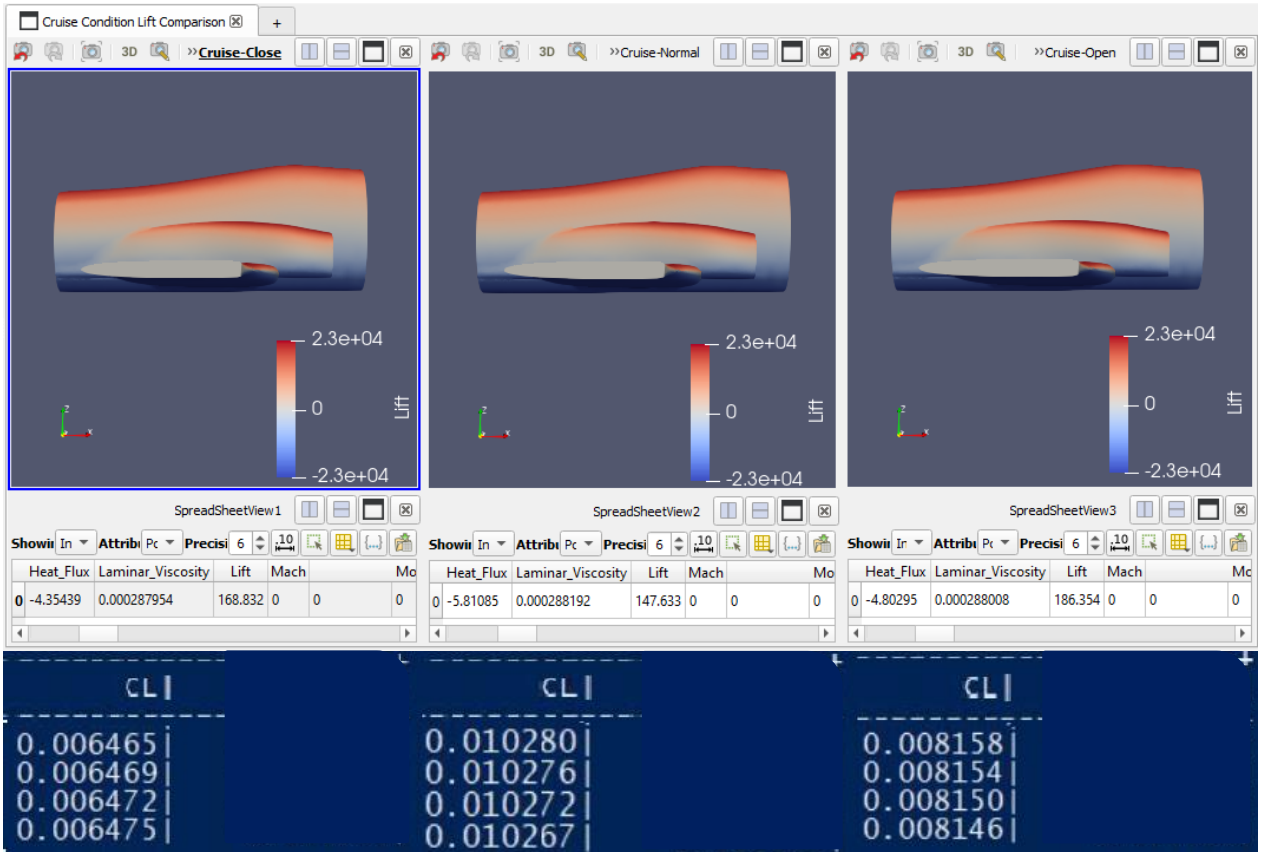

Figure 6.12. Lift Force and Lift Coefficient Comparison.

Drag, Lift Forces and Drag, Lift coefficients of Climb condition are as follows.

Close air intake:	Close air intake:
F_D=4433.93 N and C_D=0.129049	F_L=166.832 N and C_L=0.006475
Normal air intake:	Normal air intake:
F_D=4421.85 N and C_D=0.126689	F_L=147.633 N and C_L=0.010267
Open air intake:	Open air intake:
F_D=4398.11 N and C_D=0.125608	F_L=186.354 N and C_L=0.008146

From the obtained drag and lift coefficient graphs, it is seen that the open-source solver SU2 predicts the flowchart quite well in low-speed regimes. Firstly, although there are images, it would be difficult to comment directly on the images as the values are close to each other. Therefore, the numerical equivalents of the values were also calculated.
It can be understood from here that the drag force is greatest when the air intake is closed. This is the expected result because when it is closed, the air intake is modeled as a wall and increases the surface area. In addition, although it has the lowest drag coefficient, the given air conditions determined it to be the one with the highest drag effect.

The following can be said about the lift force, and this will be valid for all calculations. In the solution, the convergence criterion was determined as the drag coefficient. The iteration stopped when the drag coefficient value was lower than 1e-6. When we look at the iteration results, although the drag coefficient has converged, it has been observed that the lift coefficient has not converged yet or has converged before. In the face of this result, it is not correct to comment on the lift forces because the lift coefficient, reference area, density and velocity values change.

7. Conclusion and Recommendations

To conclude, high fidelity computations of air-intake related drag forces play a significant role in air-intake design and the general performance of aircraft. This study examines the climb and two different cruise condition and their different air-inlet configurations. To analyze the flow behavior of the climb and cruise flight conditions, a three-dimensional CFD model based on CATIA model has been developed. The influence of opening status of the air inlets was studied by varying mass flow rate for each flight conditions. From the simulation results as the air intake expands, increases amount of air taken in and decreases the drag force of the aircraft along the flow direction. This can be clearly seen from the profiles of drag force and drag coefficients. To further assure the influence of opening status of the air inlets, simulations should be carried out for higher gas velocity against the same mass flow rate. Furthermore, I analyzed climb and cruise flight condition, this study can be continued by adding landing status of the aircraft and cases considering the influence of the mass transfer and validating the simulations with experimental studies will also be considered for future work.

The drag approximations done in the design phase needed to be verified. A model of the aircraft has been analyzed with CFD and results examined to see how accurate the estimations were. A step-by-step analysis was made and then a simulation was run. The drag results of the CFD analysis meet the goal of the expected result but still not completely correct. There could be several reasons for this. Even if the mesh work meets the quality criteria, it can be considered as coarse mesh. On the other hand, there is no clear information about how big the created computational domain will be, so it should be accepted that the results are wrong. Although the reference studies were used in this study, it was not possible to compare the results because there were not experimental data on flight conditions. One of the problems encountered was that the information given with some flight conditions diverged from the results in the open-source solver after a certain point. This problem has been encountered many times. Flight conditions were created by giving free-stream temperature and free-stream pressure without using Reynolds number by trial-and-error methods. Later, experiments were made by reducing the Mach number. After the results were seen to converge, it was seen that the given flight conditions were suitable for low sub-sonic speeds, and analysis shows that the

aircraft design works well aerodynamically but also shows a few areas where the design can be improved.

The angles of attack differ in the three given flight conditions. The change of attack angles is observed in the Mach number comparison graphs as follows. As the angle of attack increased, the part where the velocity was concentrated was the downstream parts of the air intake. In the Cruise-2 flight condition, where the angle of attack was 0 degrees, the velocity distributions were uniform. Similar distributions are seen in velocity comparison charts and momentum charts.

Problems experienced.

The open-source code SU2 accepts files such as .su2 and .cgns as mesh files, but to do that another program must be used to generate these mesh files. One of the biggest problems experienced occurred at this stage. Many digital network solution programs were used, but it was seen that the most trouble-free method for three-dimensional models was to use the Fluent module of Ansys, a commercial software. The problem at this stage is that although the boundary conditions for Mesh were given via Fluent, the SU2 software read it incorrectly. The problem here was that the given boundary conditions were incorrectly as if there was only one condition. This situation was solved by using the SpaceClaim module of another commercial software, Ansys. Here, while the computational domain is being created, the boundary conditions are also given. Then, the accuracy of these boundary conditions was checked via another program (Pointwise). Until this stage, CAD drawing and boundary conditions have been given. Then, using the Mesh module of Ansys, a mesh structure that can be called coarse as the academic version allows, was applied and boundary layers are ignored. The problems encountered during the SU2 analysis were that the number of CFLs was too high and the solution exploded. I took the CFL number as 0.8, as in similar studies. Later, I changed the FREESTREAM_VEL_EQ_ONE operation given for Compressible flow non-dimensionalization to DIMENSIONAL because we had already done the non-dimensionalization of the free-stream values. Simulations were made by reducing the Mach number. After the results were seen to converge, it was seen that the given flight conditions were suitable for low sub-sonic speeds.

8. References-Citations

[1] Raymer, P. D. (2012). Aircraft Design: A Conceptual Approach (Aiaa Education Series) 5th Edition, Washington D.C: American Institute of Aeronautics and Astronautics.

[2] Aref, P., Ghoreyshi, M., Jirasek, A., & Satchell, J. M. (Ocak, 2018), CFD Validation and Flow Control of RAE-M2129 S-Duct Diffuser Using CREATETMAV Kestrel Simulation Tools, 2018 AIAA Aerospace Sciences Meeting, 5(1),31. doi:10.2514/6.2018-1512

[3] Kimberly, A. E., Frank, B. W., and Lannie D. W. (1993). Flight-determined engine exhaust characteristics of an F404 engine in an F-18 airplane, 29th AIAA/SAE/ASME/ASEE Joint Propulsion Conference, October 1993.

[4] Fluid Dynamics Panel Working Group 13. (1991) Air Intakes for High-Speed Vehicles. AGARD Advisory Report 270, retrieved from: https://apps.dtic.mil/sti/pdfs/ADA248270.pdf

[5] Menzies, Ryan D.D. (2002) Investigation of S-shaped Intake Aerodynamics Using Computational Fluid Dynamics (PhD thesis) Retrieved from http://theses.gla.ac.uk/id/eprint/1440

[6] White, M. F. (2015). Fluid Mechanics 8th Edition. New York: McGraw-Hill Education

[7] - (McGraw-Hill Series in Aeronautical and Aerospace Engineering) John D. Anderson - Modern Compressible Flow_ With Historical Perspective-McGraw-Hill (2003).

[8] "Fluid mechanics: fundamentals and applications". APA (6th ed.) Çengel, Y. A., & Cimbala, J. M. (2006). ... Çengel, Yunus A., and John M. Cimbala. 2006.

[9] Çengel, Y. A., & Boles, M. A. (2001). Thermodynamics: An ... Çengel, Yunus A., and Michael A. Boles. 2001

[10] GUNGOR, Beytullah. (Temmuz 2020). Sesalti Pitot Hava Aliği Üzerine Had Tabanli Tasarim Optimizasyonu, Bitirme Çalişmasi.

[11] HARDIE, Staffan. (2006). Drag Estimations on Experimental Aircraft Using CFD, Examensarbete i flygteknik 2006 (10 poäng). MDH.IMA.FLY.0180.2006.C.10p.Ae.

[12] TAŞKONAK, Arzu. (KASIM 2018). Uçak Kanadi Ve Muharip Uçak Aerodinamik Simülasyonlarinda Açik Kaynak Kod Kullanimi Ve Sonuçlarin Ticari Yazilim Sonuçlari İle Karşilaştirilmasi, (Phd Thesis).

[13] Three-Dimensional online model (T-45 Goshawk): https://sketchfab.com/3d-models/t45-cce874fc92f947b5adaa44158525facf

[14] https://su2code.github.io/
https://su2code.github.io/tutorials/Turbulent_ONERAM6/
[15] Online Website-Calculators

[15.1] Compressible Aerodynamics Calculator (vt.edu)
[15.2] Air Density Calculator - What is the Density of Air? (omnicalculator.com)
[15.3] Flow Rate Calculator - Finding Mass Flow Rate (omnicalculator.com)
[15.4] Air - Dynamic and Kinematic Viscosity (engineeringtoolbox.com)
[15.5] Reynolds number calculator (airfoiltools.com)
[15.6] Linear interpolation calculator (johndcook.com)
[15.7] Yüzde Hesaplama - Profesör Hesaplamacı (hesaplamaci.com)
[15.8] Air Pressure at Altitude Calculator (mide.com)
[15.9] LIFT UP (tusas.com)
[15.10] How to calculate aerodynamic forces with Paraview - YouTube

[16] ANSYS Fluent User Manual

9. Appendices

App. A: McDonnell Douglas T-45 Goshawk Dimensions

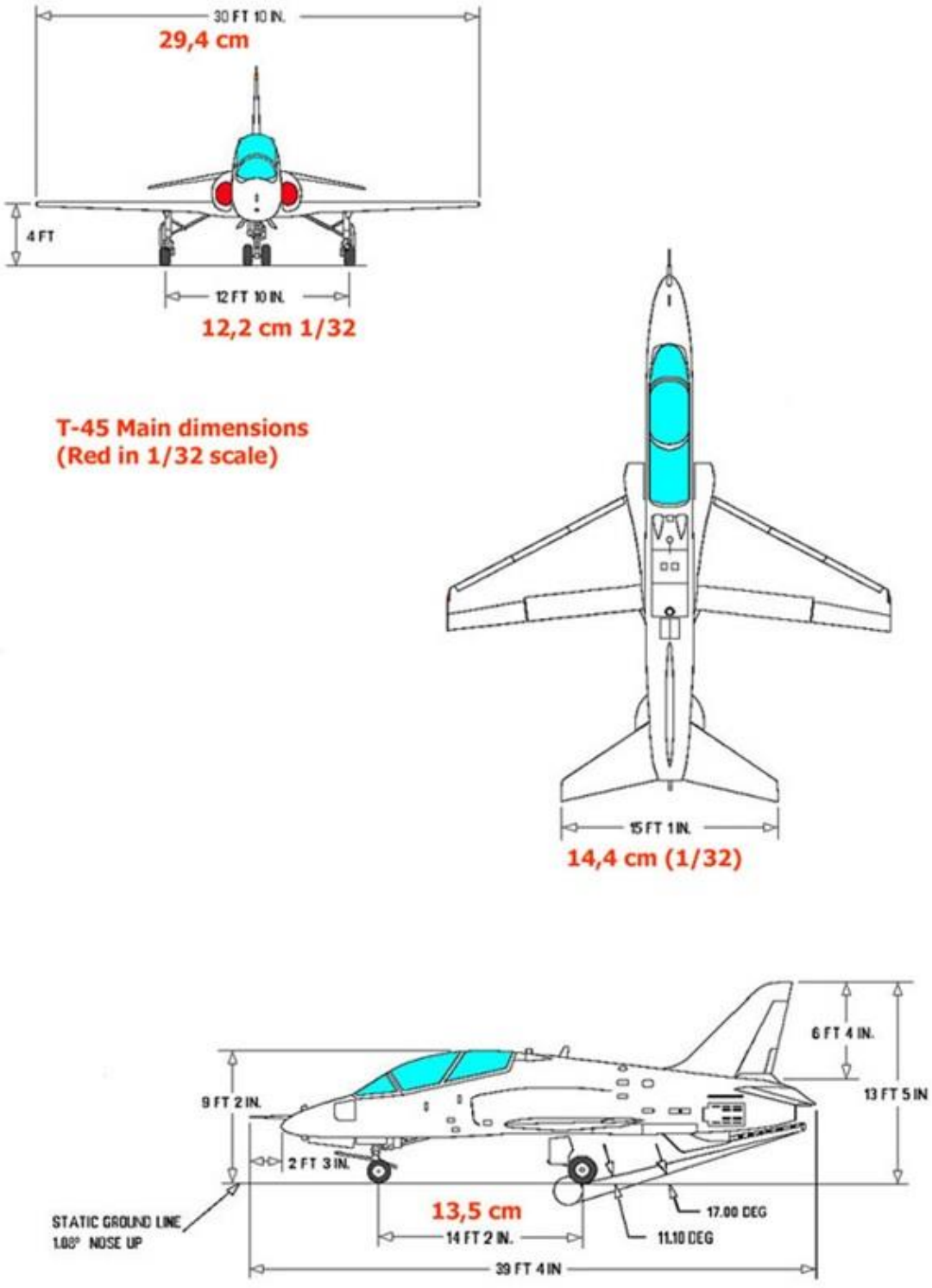

Figure A.1. McDonnell Douglas T-45 Goshawk Dimensions

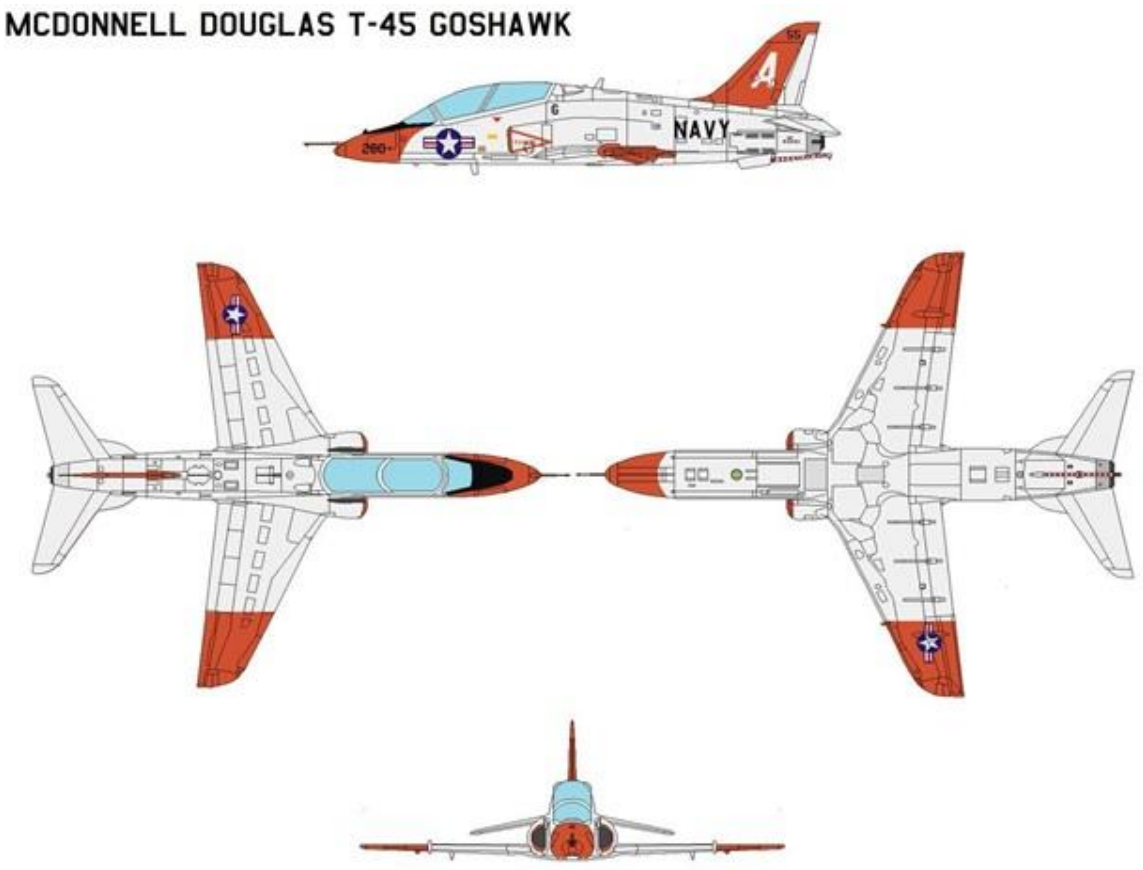

Figure A.2. Four-view of McDonnell Douglas T-45 Goshawk

Figure A.3. McDonnell Douglas T-45 Goshawk Main Modifications

App. B: Mesh structure of Fluent analysis

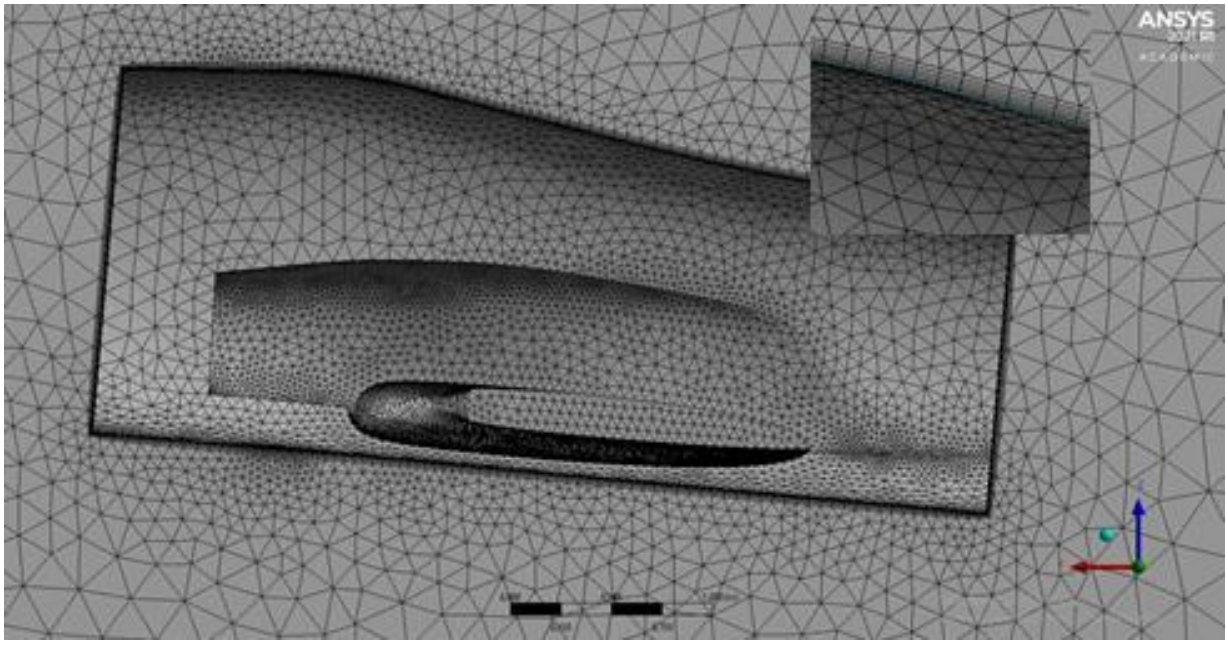

Figure B.1. Mesh structure of Fluent analysis

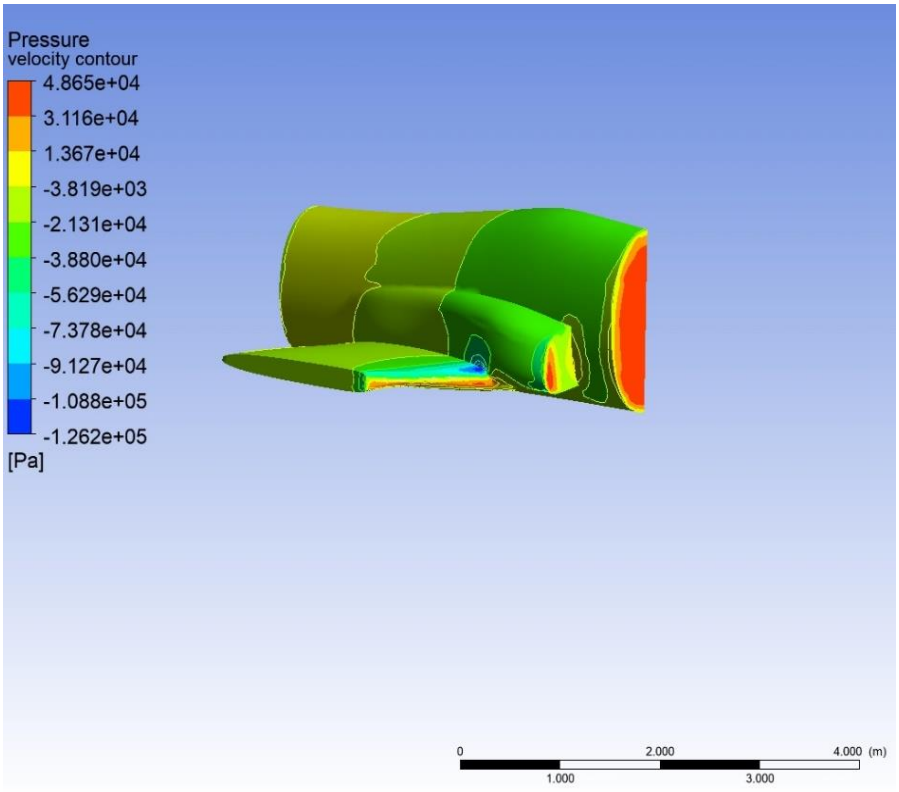

Figure B.2. Pressure contour of Fluent analysis

App. C: Climb: Velocity and Momentum comparison

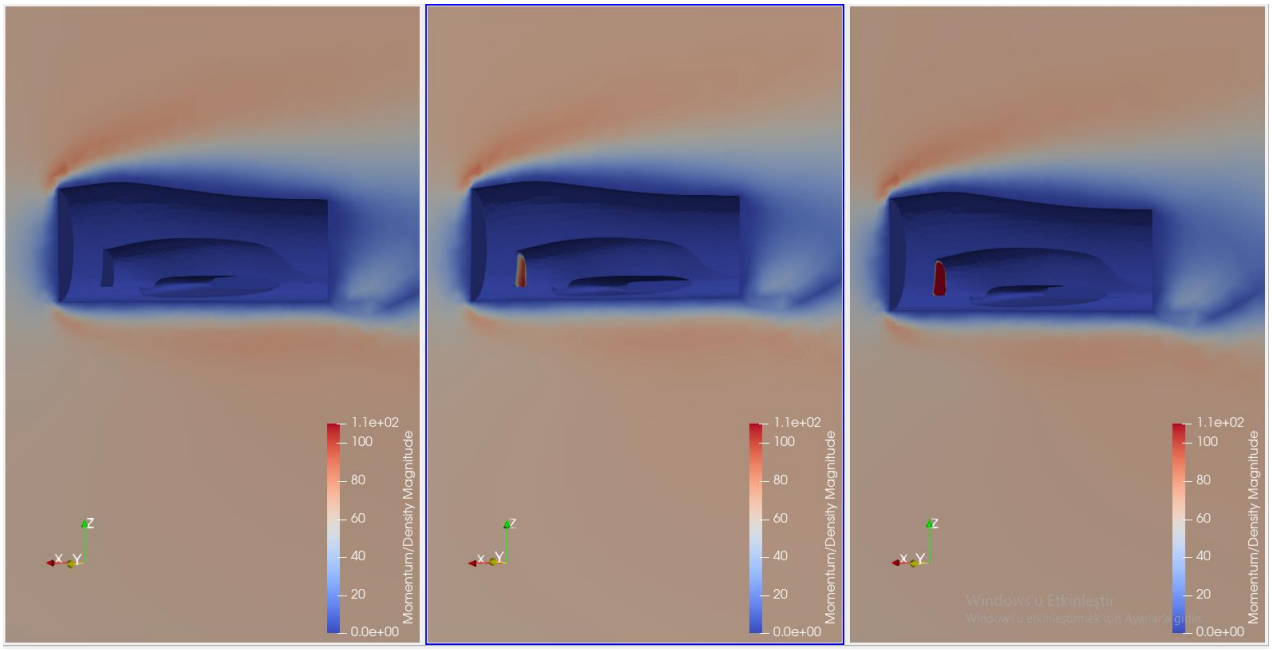

Figure C.1. Climb: Velocity Magnitude Comparison.

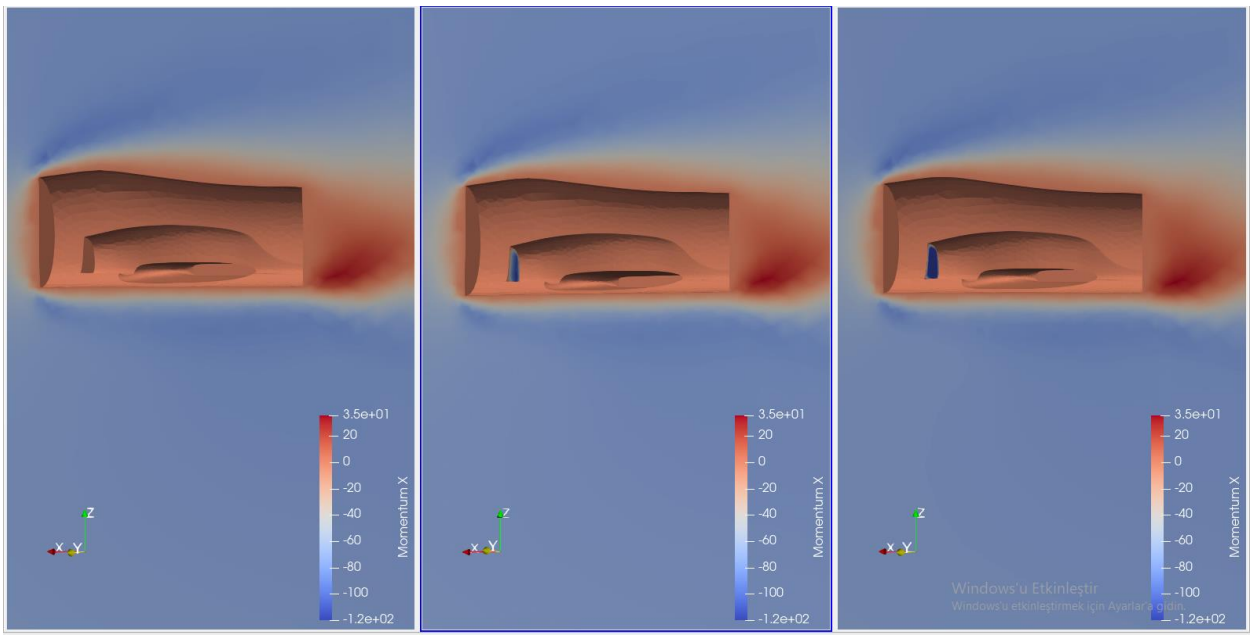

Figure C.2. Climb: Momentum-X Comparison.

App. D: Cruise-1: Velocity and Momentum comparison

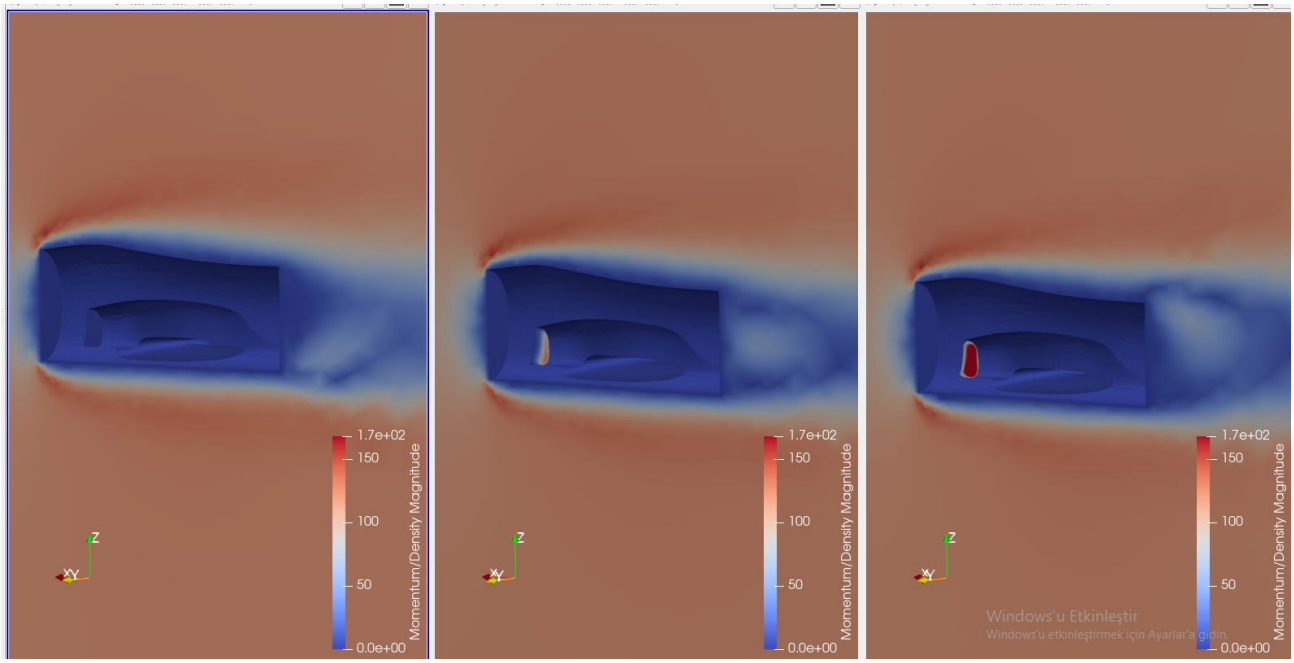

Figure D.1. Cruise-1: Velocity Magnitude Comparison.

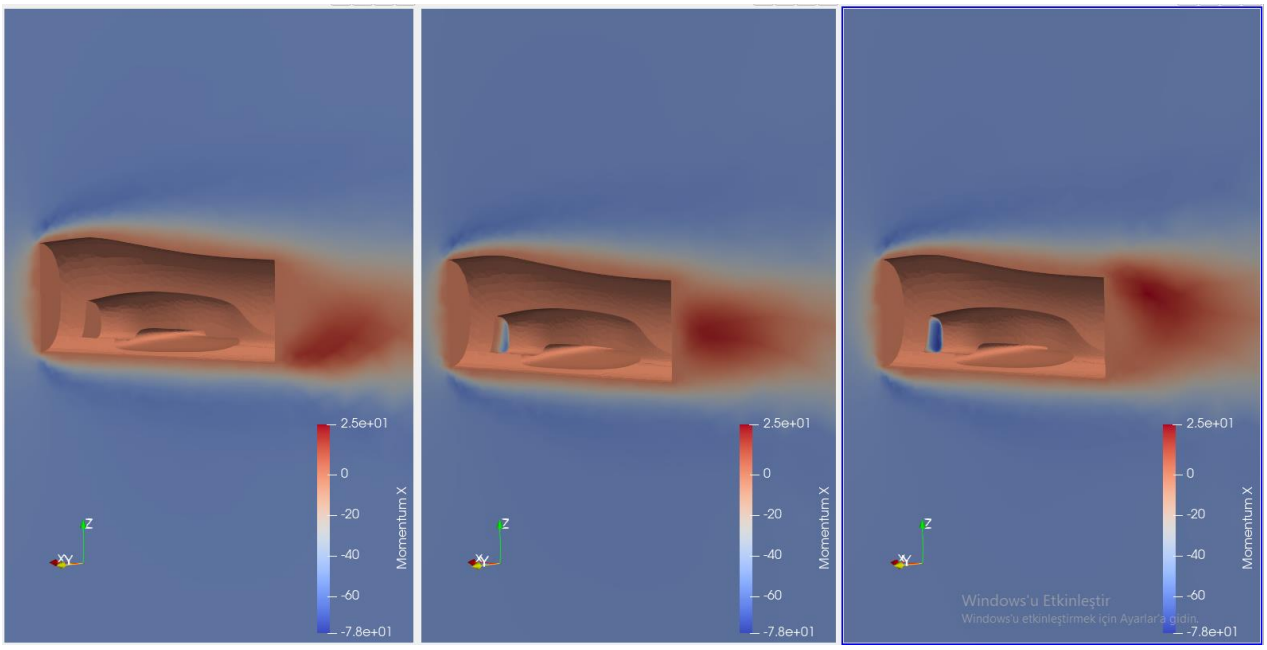

Figure D.2. Cruise-1: Momentum-X Comparison.

App. E: Cruise-2: Velocity and Momentum comparison

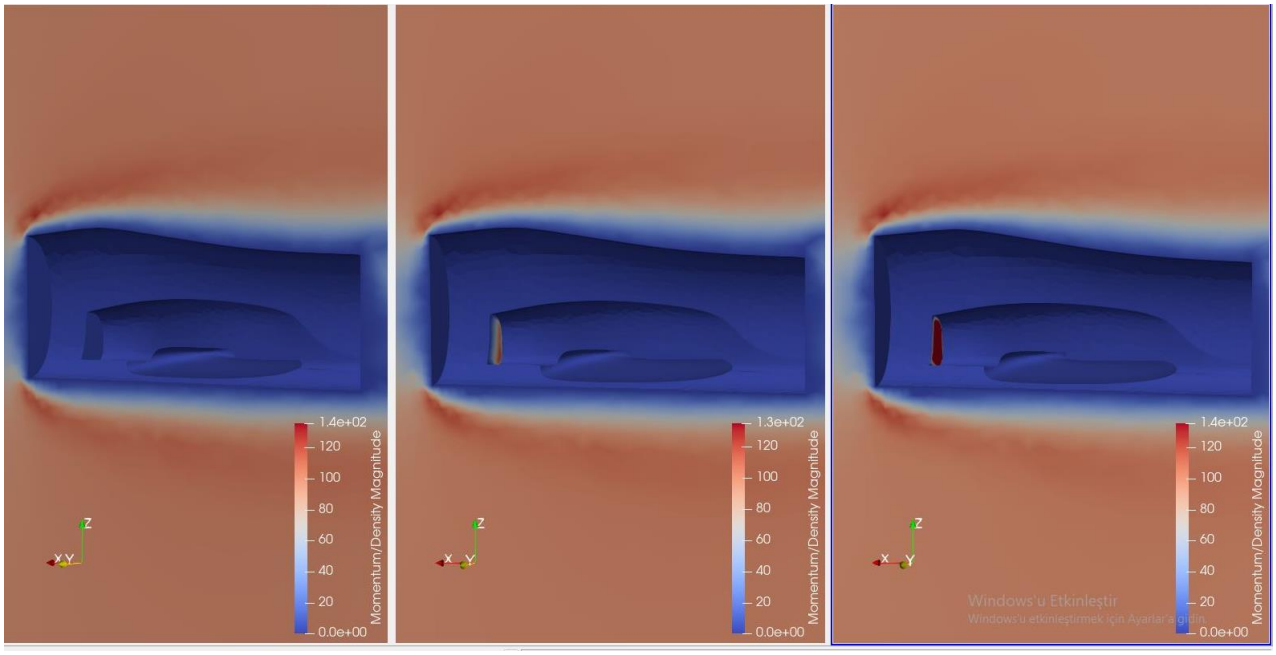

Figure E.1. Cruise-2: Velocity Magnitude Comparison.

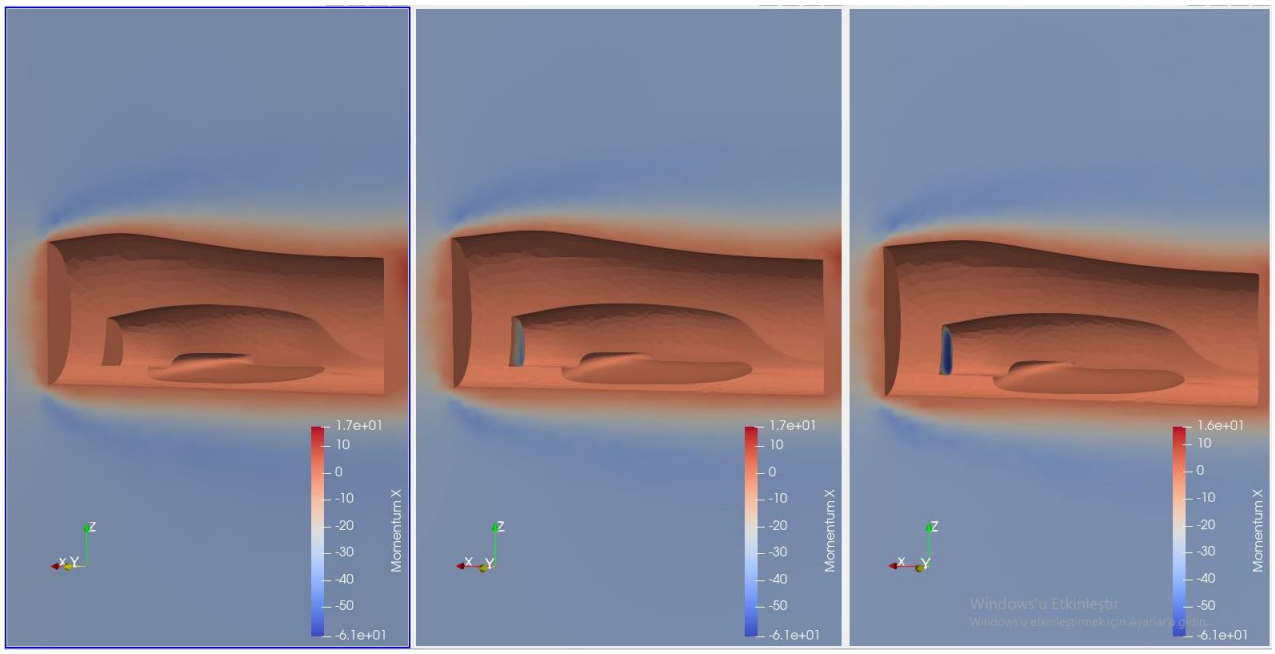

Figure E.2. Cruise-2: Momentum-X Comparison.

App. F: Summary of Configuration file

```
%%%%%%%%%%%%%%%%%%%%%%%%%%%%%%%%%%%%%%%%%%%%%%%%%%%%%%%%%%%%%%%%%%%%%%%%%%%%%%%%
% SU2 configuration file                                                        %
% Case description: T-45 Goshawk Plane Configuration File                       %
% Author: Regaib Furkan KILIÇ                                                   %
% Supervisor: Prof. Dr. Emre ALPMAN                                             %
% Institution: Marmara University                                               %
% Date: 2021.04.14                                                              %
% File Version 7.1.1 "Hi-Hatz"                                                  %
%%%%%%%%%%%%%%%%%%%%%%%%%%%%%%%%%%%%%%%%%%%%%%%%%%%%%%%%%%%%%%%%%%%%%%%%%%%%%%%%
% ------------ DIRECT, ADJOINT, AND LINEARIZED PROBLEM DEFINITION ------------%
%
SOLVER= RANS
%
KIND_TURB_MODEL= SA
% ------------------- COMPRESSIBLE FREE-STREAM DEFINITION --------------------%
%
MACH_NUMBER= X
%
AOA= X
%
SIDESLIP_ANGLE= 0.0
%
% for initializing the solution (REYNOLDS, TD_CONDITIONS)
%
INIT_OPTION= X
% ---------------------- REFERENCE VALUE DEFINITION ----------------------------%
%
REF_DIMENSIONALIZATION= DIMENSIONAL
% -------------------- BOUNDARY CONDITION DEFINITION --------------------------%
%
% Inlet boundary type (TOTAL_CONDITIONS, MASS_FLOW)
%
INLET_TYPE= X
%
MARKER_INLET= (X)
%
MARKER_OUTLET = (X)
%
MARKER_HEATFLUX= (X)
%
MARKER_PLOTTING= (X)
%
MARKER_MONITORING= (X)
% ------------ COMMON PARAMETERS DEFINING THE NUMERICAL METHOD ---------------%
%
NUM_METHOD_GRAD= GREEN_GAUSS
%
CFL_NUMBER= 0.8
%
ITER= 100000
% -------------------------- CONVERGENCE PARAMETERS --------------------------%
%
CONV_FIELD= DRAG
%
CONV_CAUCHY_EPS= 1E-6
% ------------------------ INPUT/OUTPUT INFORMATION --------------------------%
%
MESH_FILENAME= mesh.cgns
%
MESH_FORMAT= CGNS
%
SCREEN_OUTPUT= (INNER_ITER, WALL_TIME, RMS_DENSITY, RMS_NU_TILDE, LIFT, DRAG)
```

End